Abstracta

Ano XXIX - N. 03

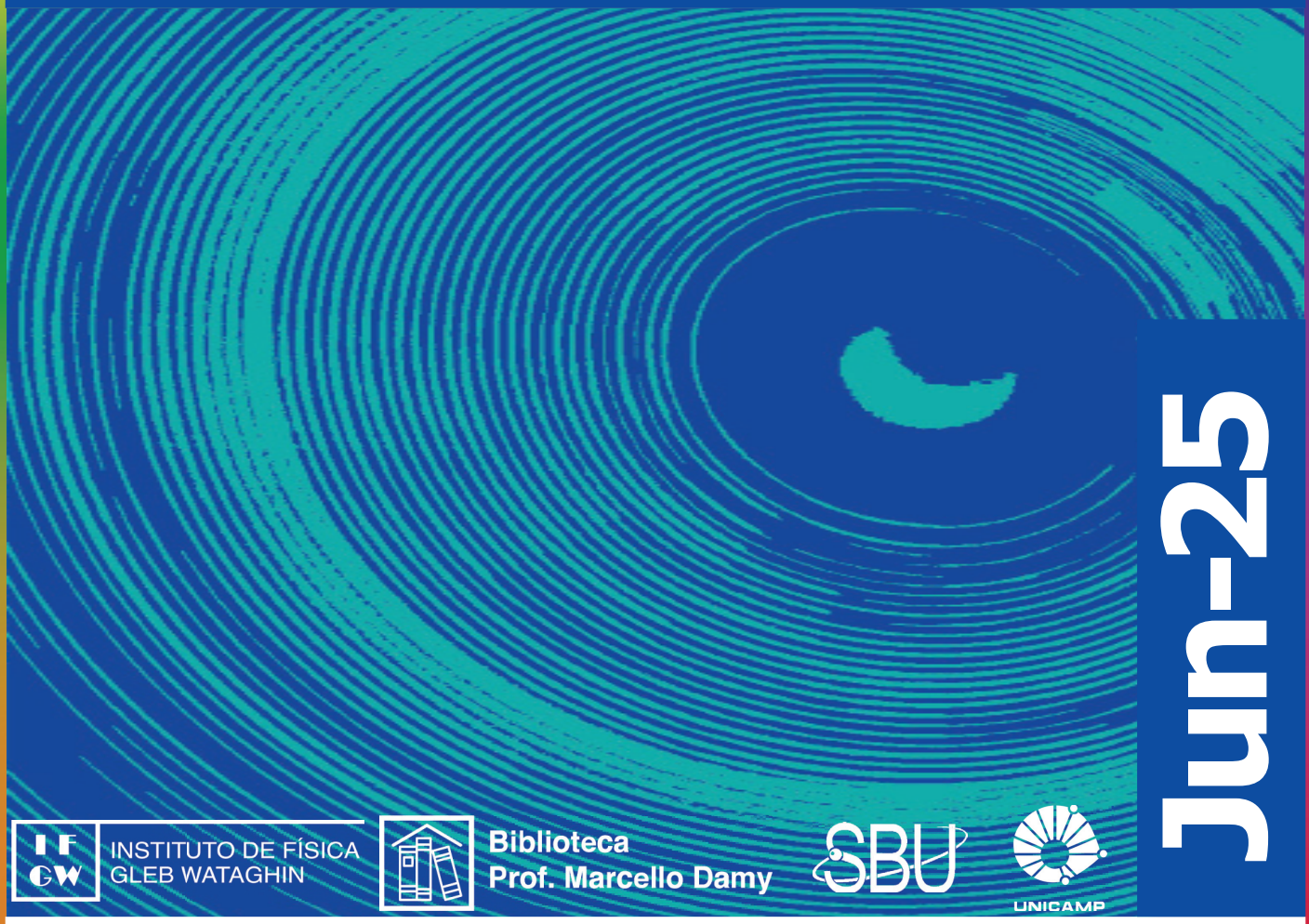

Artigos publicados

[P066-2025] "A versatile custom-built contact switching device for multi-purpose electrical transport measurements"

Oliveira, F. S.*; Canhassi, C. A. I.*; Kopelevich, Y.*; Luz, M. S. da; Santos, C. A. M. dos

This work outlines the assembly of a cost-effective and straightforward apparatus designed to automate contact switching for electrical transport measurements. We report example of applications for this custom device and showcase its versatility by employing it for electrical resistivity and Hall effect measurements following the van der Pauw method on oxygen-deficient strontium titanate single crystals, measurements on compressed bismuth using the Montgomery method, and measurements on fresh cleaved Highly Oriented Pyrolytic Graphite using a multi-line electrode configuration.

ENGINEERING RESEARCH EXPRESS 7[2], 025307, 2025. DOI: 10.1088/2631-8695/adc351

[P067-2025] "Charge Transfer of Metal Porphyrins on a NaCl Thin Film Observed by Scanning Tunneling Microscopy in the Transport Gap"

Zheng, L. Q.; Grewal, A.; Anggara, K.; **Costa, F. J. R.*;** Leon, C. C.; Kuhnke, K.; Kern, K.

Elucidating the electronic structure of organic molecules in contact with a dielectric layer is essential to understanding and controlling many important processes, such as catalysis, photochemistry, and electroluminescence. However, this challenge calls for a detailed characterization of molecule--dielectric contacts on the atomic scale. Here, we employ scanning tunneling microscopy (STM) at low temperature (4 K) in combination with ab initio calculations to investigate the subnanometer-scale electronic states of photoactive molecules on a dielectric surface. For platinum and palladium octaethylporphyrin (PtOEP and PdOEP) adsorbed on few layers of NaCl on a metal substrate, our STM imaging of them in the energy gap between the frontier orbitals demonstrates their high sensitivity to the local environment, namely, adsorption site and applied voltage. Our calculations reveal that the states in this energy gap originate from combinations of molecular orbitals far from the Fermi level and that they are affected by the extent of molecule-surface partial charge transfer, which is tuned by adsorption site and voltage in the tunnel junction.

ACS NANO 19[19], p. 18357-18363, 2025. DOI: 10.1021/acsnano.5c01235

[P068-2025] "Chemical Sensors and Biosensors for Point-of--Care Testing of Pets: Opportunities for Individualized Diagnostics of Companion Animals"

Fonseca, W. T.; Vello, T. P.; Lelis, G. C.; Deleigo, A. V. F.; Takahira, R. K.; Martinez, D. S. T.; **Oliveira, R. F. de***

Point-of-care testing (POCT) is recognized as one of the most disruptive medical technologies for rapid and decentralized diagnostics. Successful commercial examples include portable glucose meters, pregnancy tests, and COVID-19 self-tests. However, compared to advancements in human healthcare, POCT technologies for companion animals (pets) remain significantly underdeveloped. This Review explores the latest advancements in pet POCT and examines the challenges and opportunities in the field for individualized diagnostics of cats and dogs. The most frequent diseases and their respective biomarkers in blood, urine, and saliva are discussed. We examine key strategies for developing the next-generation POCT devices by harnessing the potential of selective (bio)receptors and high-performing transducers such as lateral flow tests and electrochemical (bio)sensors. We also present the most recent research initiatives and the successful commercial pet POCT technologies. We discuss future trends in the field, such the role of biomarker discovery and development of wearable, implantable, and breath sensors. We believe that advancing pet POCT technologies benefits not only animals but also humans and the environment, supporting the One Health approach.

ACS SENSORS 10[5], p. 3222-3238, 2025. DOI: 10.1021/acssensors.4c03664

[P069-2025] "Chiral oscillations in finite time quantum field theory"

Blasone, M.; Giacosa, F.; Smaldone, L.; **Torrieri, G.***

We demonstrate how chiral oscillations of a massive Dirac field can be described within quantum field theory using a finite-time interaction picture approach, where the mass term in the Lagrangian is treated as a perturbative coupling between massless fields of definite chirality. We derive the formula for chiral oscillations at the fourth order in the perturbative expansion, obtaining a result consistent with the formula derived by means of other methods. Furthermore, we illustrate how the perturbative framework of chiral oscillations can effectively describe production processes where an electron must exhibit both left chirality and positive helicity, as in decay pi-->e-+v-e. Finally, we argue that, in this perturbative view, chiral oscillations are also essential for detecting the decay products in such processes.

EUROPEAN PHYSICAL JOURNAL C 85[5] 523, 2025. DOI: 10.1140/epjc/s10052-025-14165-2

[P070-2025] "Coherent Feedback Control of Indirectly Coupled Mode Multipartite Entanglement in a Cavity Opto-Magnomechanical System"

Sohail, A.*; Amazioug, M.; Singh, S. K.; Chabar, N.; Ahmed, R.; **Oliveira, M. C. de***

This study is based on a theoretical proposal for the generation and enhancement of multipartite entanglements of indirectly coupled modes using the coherent feedback loop scheme. The coherent feedback-control mechanism that is presented here significantly improves the bipartite and tripartite entanglements among the indirectly coupled modes. The numerical study shows that the entanglements can be sufficiently tuned by the effective couplings and the reflective parameter of the beam splitter. In addition, the robustness and survival of the generated entanglement in the proposed system have shown to be significantly dependent on the reflectivity parameter. The existence of a genuine tripartite entanglement state in the dynamical state of the system is proven. Finally, the effect of the reflective parameter on three different tripartite entanglements is observed. The findings pave the way for tuning and enhancing multipartite entanglements of indirectly coupled modes in current cavity Opto-magnomechanical systems and may have various vital applications in quantum information.

ANNALEN DER PHYSIK, 2025. DOI: 10.1002/andp.202400375 Early Access Date: MAY 2025

[P071-2025] "Common femtoscopic hadron-emission source in pp collisions at the LHC"

Acharya, S.; Adamová, D.; Rinella, G. A.; **Chinellato, D. D.*; Guardiano, G. G.*; Liveraro, G. S. S.*; Takahashi, J.***; et al.
ALICE Collaboration

The femtoscopic study of pairs of identical pions is particularly suited to investigate the effective source function of particle emission, due to the resulting Bose-Einstein correlation signal. In small collision systems at the LHC, pp in particular, the majority of the pions are produced in resonance decays, which significantly affect the profile and size of the source. In this work, we explicitly model this effect in order to extract the primordial source in pp collisions at root s = 13 TeV from charged pi-pi correlations measured by ALICE. We demonstrate that the assumption of a Gaussian primordial source is compatible with the data and that the effective source, resulting from modifications due to resonances, is approximately exponential, as found in previous measurements at the LHC. The universality of hadron emission in pp collisions is further investigated by applying the same methodology to characterize the primordial source of K-p pairs. The size of the primordial source is evaluated as a function of the transverse mass (m(T)) of the pairs, leading to the observation of a common scaling for both pi-pi and K-p, suggesting a collective effect. Further, the present results are compatible with the mT scaling of the p-p and p-Lambda primordial source measured by ALICE in high multiplicity pp collisions, providing additional evidence for the presence of a common emission source for all hadrons in small collision systems at the LHC. This will allow the determination of the source function for any hadron-hadron pairs with high precision, granting access to the properties of the possible final-state interaction among pairs of less abundantly produced hadrons, such as strange or charmed particles.

EUROPEAN PHYSICAL JOURNAL C 85[2], 198, 2025. DOI: 10.1140/epjc/s10052-025-13793-y

[P072-2025] "Computational Characterization of the Recently Synthesized Pristine and Porous 12-Atom-Wide Armchair Graphene Nanoribbon"

Gomes, D. S.*; Felix, I. M.; Radel, W. F.; Dias, A. C.; Ribeiro Junior, L. A.; Pereira Junior, M. L.

Recently synthesized porous 12-atom-wide armchair graphene nanoribbons (12-AGNRs) exhibit tunable properties through periodic porosity, enabling precise control over their electronic, optical, thermal, and mechanical behavior. This work presents a comprehensive theoretical characterization of pristine and porous 12-AGNRs based on density functional theory (DFT) and molecular dynamics simulations. DFT calculations reveal substantial electronic modifications, including band gap widening and the emergence of localized states. Analyzed within the Bethe-Salpeter equation framework, the optical properties highlight strong excitonic effects and significant absorption shifts. Thermal transport simulations indicate a pronounced reduction in conductivity due to enhanced phonon scattering at the nanopores. At the same time, MD-based mechanical analysis shows decreased stiffness and strength while maintaining the structural integrity. Despite these modifications, porous 12-AGNRs remain mechanically and thermally stable. These findings establish porosity engineering as a powerful strategy for tailoring graphene nanoribbons' functional properties, reinforcing their potential for nanoelectronic, optoelectronic, and thermal management applications.

NANO LETTERS 25[21], p. 8596-8603, 2025. DOI: 10.1021/acs.nanolett.5c01319

[P073-2025] "Constraints on the Higgs boson self-coupling from the combination of single and double Higgs boson production in proton-proton collisions at √s=13 TeV"

Hayrapetyan, A.; Tumasyan, A.; Adam, W.; **Chinellato, J. A.***; et al.
CMS Collaboration

The Higgs boson (H) trilinear self-coupling, lambda(3), is constrained via its measured properties and limits on the HH pair production using the proton-proton collision data collected by the CMS experiment at root s = 13 TeV. The combination of event categories enriched in single-H and HH events is used to measure k(lambda), defined as the value of lambda(3) normalized to its standard model prediction, while simultaneously constraining the Higgs boson couplings to fermions and vector bosons. Values of k(lambda) outside the interval -1.2 < k(lambda) < 7.5 are excluded at 2 sigma confidence level, which is compatible with the expected range of -2.0< k(lambda) < 7.7 under the assumption that all other Higgs boson couplings are equal to their standard model predicted values. Relaxing the assumption on the Higgs couplings to fermions and vector bosons the observed (expected) k(lambda) interval is constrained to be within -1.4 < k(lambda) < 7.8 (-2.3 < k(lambda) < 7.8) at 2 sigma confidence level.

PHYSICS LETTERS B 861, 139210, 2025. DOI: 10.1016/j.physletb.2024.139210

[P074-2025] "Cross-Polarized Stimulated Brillouin Scattering in Lithium Niobate Waveguides"

Rodrigues, C. C.*; Schilder, N. J.*; Zurita, R. O.*; Magalhaes, L. S.; Shams-Ansari, A.; **Santos, F. J. L. dos*; Paiano, O. M.*; Alegre, T. P. M.***; Loncar, M.; **Wiederhecker, G. S.***

We report on the experimental demonstration of cross-polarization backward stimulated Brillouin scattering (BSBS) in lithium niobate on insulator (LNOI) waveguides. Performing polarization-sensitive pump and probe measurements, we captured both intra-and intermodal scattering between counter-propagating fundamental optical modes. Remarkably, cross-polarization scattering achieved SBS gains that exceeded GB = 80 m-1 W-1. This substantial gain not only broadens the utility of polarization in SBS but also paves the way for high-performance devices, including ultranarrowband lasers, robust broadband nonreciprocal devices, RF filters, and microwave-to-optical converters.

PHYSICAL REVIEW LETTERS 134[11], 113601, 2025. DOI: 10.1103/PhysRevLett.134.113601

[P075-2025] "Dark Energy Survey Year 3 results: Simulation-based cosmological inference with wavelet harmonics, scattering transforms, and moments of weak lensing mass maps. II. cosmological results"

Gatti, M.; Campailla, G.; **Navarro-Alsina, A.***; et al.

We present a simulation-based cosmological analysis using a combination of Gaussian and non-Gaussian statistics of the weak lensing mass (convergence) maps from the first three years of the Dark Energy Survey. We implement the following: (1) second and third moments; (2) wavelet phase harmonics; (3) the scattering transform. Our analysis is fully based on simulations, spans a space of seven w Cold Dark Matter (wCDM) cosmological parameters, and forward models the most relevant sources of systematics inherent in the data: masks, noise variations, clustering of the sources, intrinsic alignments, and shear and redshift calibration. We implement a neural network compression of the summary statistics, and we estimate the parameter posteriors using a simulation-based inference approach.Including and combining different non-Gaussian statistics is a powerful tool that strongly improves constraints over Gaussian statistics (in our case, the second moments); in particular, the figure of merit (S-8; Omega(m)) is improved by 70% (ACDM) and 90% (wCDM).

When all the summary statistics are combined, we achieve a 2% constraint on the amplitude of fluctuations parameter S-8 equivalent to 68(Omega(m)/0.3)(0.5,) obtaining S-8 = 0.794 + 0.017 (ACDM) and S-8 = 0.817 + 0.021 (wCDM), and a similar to 10% constraint on Omega(m), obtaining Omega(m) = 0.259 + 0.025 (ACDM) and Omega(m) = 0.273 + 0.029 (wCDM). In the context of the wCDM scenario, these statistics also strengthen the constraints on the parameter w, obtaining w < -0.72. The constraints from different statistics are shown to be internally consistent (with a p-value>0.1 for all combinations of statistics examined). We compare our results to other weak lensing results from the first three years of the Dark Energy Survey data, finding good consistency; we also compare with results from external datasets, such as Planck constraints from the cosmic microwave background, finding statistical agreement, with discrepancies no greater than <2.2 sigma.

PHYSICAL REVIEW D 111[6], 063504, 2025. DOI: 10.1103/PhysRevD.111.063504

[P076-2025] "Differential cross section measurements for the production of top quark pairs and of additional jets using dilepton events from pp collisions at √s=13 TeV"

Tumasyan, A.; Adam, W.; Andrejkovic, J. W.; **Chinellato, J. A.*;** et al.
CMS Collaboration

Differential cross sections for top quark pair (t (t) over bar) production are measured in proton-proton collisions at a center-of-mass energy of 13 TeV using a sample of events containing two oppositely charged leptons. The data were recorded with the CMS detector at the CERN Large Hadron Collider and correspond to an integrated luminosity of 138 fb(-1). The differential cross sections are measured as functions of kinematic observables of the t (t) over bar system, the top quark and antiquark and their decay products, as well as of the number of additional jets in the event. The results are presented as functions of up to three variables and are corrected to the parton and particle levels. When compared to standard model predictions based on quantum chromodynamics at different levels of accuracy, it is found that the calculations do not always describe the observed data. The deviations are found to be largest for the multi-differential cross sections.

JOURNAL OF HIGH ENERGY PHYSICS [2], 064, 2025. DOI: 10.1007/JHEP02(2025)064

[P077-2025] "Doniach Lattice Gas on Bipartite Lattices in the Mean-Field Approximation"

Vignoto, C. P. B.*; Tamashiro, M. N.*

The Doniach lattice gas (DLG) consists of a statistical model that can be mapped into a spin-1 Ising model with highly degenerate single-site states and the inclusion-using the nomenclature of the analogous magnetic model-of dipole-quadrupole interactions, besides the usual dipole-dipole, Zeeman-effect and crystal-field interactions. Its formulation was motivated aiming at the study of phase transitions in supramolecular structures of zwitterionic phospholipids, in particular, allowing an alternative description of density fluctuations in the system, already included in a certain class of lattice models (Nagle, J. F. J. Chem. Phys. 1973, 58, 252; Nagle, J. F. J. Chem. Phys. 1975, 63, 1255), but not considered in previous proposals of Ising-type models (Doniach, S. J. Chem. Phys. 1978, 68, 4912). In this work, we investigate the DLG model, considering the division of the system into two interpenetrating sublattices, under the framework of the mean-field approximation. This analysis of the model on bipartite lattices allowed the investigation of staggered phases, which were overlooked in the first analysis of the model in the mean-field approach (Guidi, H. S.; Henriques, V. B. Phys. Rev. E 2014, 90, 052705), precisely because it was only assumed the presence of uniform phases, i.e., without splitting the system into two distinct sublattices. However, such staggered phases were observed for this model in the pair approximation on bipartite lattices (de Oliveira, F. O.; Tamashiro, M. N. Phys. Rev. E 2019, 99, 012147; de Oliveira, F. O.; Tamashiro, M. N. Langmuir 2019, 35, 3848). Throughout the work, in addition to the staggered phase, we also observed intermediate topologies of representative phase diagrams (mu/z, t/z), which explain the development of the main topologies as we change the parameters (l , k) associated with the effective Hamiltonian interactions. Finally, we perform a parameter fitting between theoretical results and isothermal compression experimental data for the phospholipid 1,2-dimyristoyl-sn-glycero-3-phosphocholine (DMPC), allowing also a comparison between the fittings obtained using the mean-field and the pair approximations.

LANGMUIR 41[19], p. 11838-11853, 2025. DOI: 10.1021/acs.langmuir.4c04225

[P078-2025] "Electric-Field Control of Photon Indistinguishability in Cascaded Decays in Quantum Dots"

Undeutsch, G.; Aigner, M.; Garcia Jr., A. J.; Reindl, J.; Peter, M.; Mader, S.; Weidinger, C.; **Silva, S. F. C. da***; Manna, S.; Schöll, E.; Rastelli, A.

Photon indistinguishability, entanglement, and antibunching are key ingredients in quantum optics and photonics. Decay cascades in quantum emitters offer a simple method to create entangled-photon-pairs with negligible multipair generation probability. However, the degree of indistinguishability of the photons emitted in a cascade is intrinsically limited by the lifetime ratio of the involved transitions. Here we show that, for the biexciton-exciton cascade in a quantum dot, this ratio can be widely tuned by an applied electric field. Hong-Ou-Mandel interference measurements of two subsequently emitted biexciton photons show that their indistinguishability increases with increasing field, following the theoretically predicted behavior. At the same time, the emission line width stays close to the transform-limit, favoring applications relying on the interference among photons emitted by different sources.

NANO LETTERS 25[17], p. 7121-7127, 2025. DOI: 10.1021/acs.nanolett.5c01354

[P079-2025] "Emergence of X states in a quantum impurity model"

Cavalcante, M. F.*; Bonanca, M. V. S.*; Miranda, E.*; Deffner, S.

In the present work, we demonstrate the emergence of X states in the long-time response of a locally perturbed many-body quantum impurity model. The emergence of the double-qubit state is heralded by the lack of decay of the response function as well as the out-of-time order correlator, signifying the trapping of excitations and hence information in edge modes. Surprisingly, after carrying out a quantum information theory characterization, we show that such states exhibit genuine quantum correlations.

PHYSICAL REVIEW RESEARCH 7[2], L022027, 2025. DOI: 10.1103/PhysRevResearch.7.L022027

[P080-2025] "First observation of antiproton annihilation at rest on argon in the LArIAT experiment"

Basque, V.; Acciarri, R.; Asaadi, J.; **Kemp, E.***; et al.
LArIAT Collaboration

We report the first observation and measurement of antiproton annihilation at rest on argon track and shower multiplicities and particle identification conducted with the LArIAT experiment. Stopping antiprotons from the Fermilab Test Beam Facility's charged particle test beam are identified using beamline instrumentation and LArIAT's liquid argon time projection chamber (LArTPC). The charged particle multiplicity from the annihilation vertex is manually evaluated via hand scanning, yielding a mean of 3.2 + 0.4 tracks and a standard deviation of 1.3 tracks, consistent with a semiautomated reconstruction resulting in 2.8 + 0.4 tracks and a standard deviation of 1.2 tracks. Both methods are consistent with Monte Carlo simulations within statistical uncertainty. The shower multiplicities and particle identification for outgoing tracks are also consistent with Geant4 model predictions. These results, obtained from a low-statistics sample, provide a foundation for higher-statistics studies in larger LArTPCs, which could refine modeling of intranuclear annihilation on argon and inform scenarios such as neutron-antineutron oscillations.

PHYSICAL REVIEW D 111[9], 094031, 2025. DOI: 10.1103/PhysRevD.111.094031

[P081-2025] "First observation of strange baryon enhancement with effective energy in pp collisions at the LHC"

Acharya, S.; Agarwal, A.; **Guardiano, G. G.*; Liveraro, G. S. S.*; Takahashi, J.***; et al.
ALICE Collaboration

The production of (multi-)strange hadrons is measured at midrapidity in proton-proton collisions at root s = 13 TeV as a function of the local charged-particle multiplicity in the pseudorapidity interval |eta| < 0.5 and of the very-forward energy measured by the ALICE Zero-Degree Calorimeters. The latter provides information on the effective energy, i.e. the energy available for particle production in the collision once subtracted from the centre-of-mass energy. The yields of K-S(0), Lambda + (Lambda) over bar, and Xi(-) + (Xi) over bar (+) per charged-particle increase with the effective energy. In addition, this work exploits a multi-differential approach to decouple the roles of local multiplicity and effective energy in such an enhancement. The results presented in this article provide new insights into the interplay between global properties of the collision, such as the initial available energy in the event, and the locally produced final hadronic state, connected to the charged-particle multiplicity at midrapidity. Notably, a strong increase of strange baryon production with effective energy is observed for fixed charged-particle multiplicity at midrapidity. These results are discussed within the context of existing phenomenological models of hadronisation implemented in different tunes of the PYTHIA 8 event generator.

JOURNAL OF HIGH ENERGY PHYSICS 3, 29, 2025. DOI: 10.1007/JHEP03(2025)029

[P082-2025] "Flavor composition of supernova neutrinos"

Capanema, A.; **Porto, Y.***; Saez, M. M.

Predicting the flavor composition of neutrinos from supernovae is a challenging task, primarily due to the high neutrino densities at their core. In such an environment, neutrino self-interactions give rise to collective effects that have dramatic yet poorly understood consequences for their flavor evolution. In this paper, however, we show that standard matter effects in the outer layers of supernovae can significantly constrain the flavor composition of the neutrino flux. We assume that, since a large number of neutrinos undergo different evolutions within the core, their state upon entering the Mikheyev-Smirnov-Wolfensteindominated region is affected by decoherence. This assumption simplifies the problem and suggests that the fraction of neutrinos with electron flavor reaching Earth, denoted as f nu e, is constrained to be less than 0.5 for all energies throughout the emission phase in the case of normal mass ordering. In contrast, for inverted mass ordering, we anticipate neutrinos arriving in near flavor equipartition (f nu e approximate to 1/3). These predictions, and consequently their underlying assumptions, could be tested by future observations and may provide valuable insights into the properties of neutrino fluxes emerging from supernovae.

PHYSICAL REVIEW D 111[10], 103021, 2025. DOI: 10.1103/PhysRevD.111.103021

[P083-2025] "Girth and groomed radius of jets recoiling against isolated photons in lead-lead and proton-proton collisions at √sNN=5.02 TeV"

Hayrapetyan, A.; Tumasyan, A.; Adam, W.; **Chinellato, J. A.***; et al.
CMS Collaboration

This Letter presents the first measurements of the groomed jet radius R-g and the jet girth g in events with an isolated photon recoiling against a jet in lead-lead (PbPb) and proton-proton (pp) collisions at the LHC at a nucleon-nucleon center-of-mass energy of 5.02 TeV. The observables R-g and g provide a quantitative measure of how narrow or broad a jet is. The analysis uses PbPb and pp data samples with integrated luminosities of 1.7 nb(-1) and 301 pb(-1), respectively, collected with the CMS experiment in 2018 and 2017. Events are required to have a photon with transverse momentum p(T)(gamma) > 100 GeV and at least one jet back-to-back in azimuth with respect to the photon and with transverse momentum p(T)(jet) such that p(T)(jet)/p(T)(gamma) > 0.4. The measured R-g and g distributions are unfolded to the particle level, which facilitates the comparison between the PbPb and pp results and with theoretical predictions. It is found that jets with p(T)(jet)/p(T)(gamma) > 0.8, i.e., those that closely balance the photon p(T)(gamma), are narrower in PbPb than in pp collisions. Relaxing the selection to include jets with p(T)(jet)/p(T)(gamma) > 0.4 reduces the narrowing of the angular structure of jets in PbPb relative to the pp reference. This shows that selection bias effects associated with jet energy loss play an important role in the interpretation of jet substructure measurements.

PHYSICS LETTERS B 861, 139088, 2025. DOI: 10.1016/j.physletb.2024.139088

[P084-2025] "Hydrogen evolution reactions using 3D printed composites of copper with graphene and hexagonal boron nitride"

Das, R.; **Benjamim, R.***; Kotal, M.; Machado, L.; **Galvao, D. S.***; Tiwary, C. S.

The design of scalable, efficient electrocatalysts is essential for green hydrogen production. Here, we employed direct ink writing (DIW) 3D printing to fabricate Cu-based composites with graphene (Gr) and hexagonal boron nitride (h-BN), utilizing precise porosity control and interface engineering for enhanced hydrogen evolution reaction (HER) performance. The DIW-printed Cu-Gr composite outperforms Cu-hBN and pristine Cu, achieving an overpotential of 129 mV at 20 mA cm-2, a Tafel slope of 125 mV dec-1, and excellent stability over 10 hours. Improved conductivity, charge transport, and active site exposure drive superior catalytic activity. Computational studies confirm that Gr (or h-BN) enhances the adsorption enthalpy, promoting catalytic interactions.

This work highlights DIW-printed Cu-Gr composites as scalable, self-standing, and sustainable HER electrocatalysts.

CHEMICAL COMMUNICATIONS, 2025. DOI: 10.1039/d5cc01464f
Early Access Date: MAY 2025

[P085-2025] "Impact of the surface density of paraTerphenyl films on the Vacuum Ultra Violet light conversion efficiency"

Pagliuso, L. L.*; Mendonca, A. P. A.*; Santos, R. F.*; Pilon, T. B.*; Machado, A. A.*; Segreto, E.*

This work studies the efficiency of paraTerphenyl (PTP) films for converting Vacuum Ultra Violet (VUV) light, as a function of their thickness. The PTP films were coated on microscope glasses using the vacuum evaporation technique. The arrangement of the glasses within the evaporation chamber was done to ensure different levels of PTP deposition, with those closer to the center having higher mass values. Surface density measurements were conducted by pre-and post-deposition weighing of the glasses. Relative measurements of the conversion efficiency with respect to a reference sample were done in a vacuum monochromator with a deuterium lamp. The goal of this set of experiments is to understand the impact of PTP thickness on film conversion efficiency. Furthermore, the study employs Profilometry and Optical Microscopy measurements to verify if structural and morphological effects can impact the efficiency of the film. Results indicate that PTP resembles TPB by showing a small change in efficiency due to surface density variations, inside the explored range of thickness.

JOURNAL OF INSTRUMENTATION 20[5], C05027, 2025. DOI: 10.1088/1748-0221/20/05/C05027

[P086-2025] "Inference of the Mass Composition of Cosmic Rays with Energies from 1018.5 to 1020 eV Using the Pierre Auger Observatory and Deep Learning"

Halim, A. A.; Abreu, P.; Aglietta, M.; **Bonneau Arbeletche, L.*; Chinellato, J. A.*; Dobrigkeit, C.*; Fauth, A. C.*; Machado Payeras, A.*; Reginatto Akim, J. V.***; et al.
Pierre Auger Collaboration

We present measurements of the atmospheric depth of the shower maximum X-max, inferred for the first time on an event-by-event level using the surface detector of the Pierre Auger Observatory. Using deep learning, we were able to extend measurements of the X-max distributions up to energies of 100 EeV (10(20) eV), not yet revealed by current measurements, providing new insights into the mass composition of cosmic rays at extreme energies. Gaining a 10-fold increase in statistics compared to the fluorescence detector data, we find evidence that the rate of change of the average X-max with the logarithm of energy features three breaks at 6.5 +/- 0.6(stat) +/- 1(syst) EeV, 11 +/- 2(stat)+/- 1(syst)EeV, and 31 +/- 5(stat)+/- 3(syst)EeV, in the vicinity to the three prominent features (ankle, instep, suppression) of the cosmic-ray flux. The energy evolution of the mean and standard deviation of the measured X-max distributions indicates that the mass composition becomes increasingly heavier and purer, thus being incompatible with a large fraction of light nuclei between 50 and 100 EeV.

PHYSICAL REVIEW LETTERS 134[2], 021001, 2025. DOI: 10.1103/PhysRevLett.134.021001

[P087-2025] "Investigating Λ baryon production in p-Pb collisions in jets and the underlying event using angular correlations"

Acharya, S.; Adamova, D.; Agarwal, A.; **Chinellato, D. D.*; Guardiano, G. G.*; Liveraro, G. S. S.*; Takahashi, J.***; et al.
ALICE Collaboration

First measurements of hadron- Lambda(h-Lambda) azimuthal angular correlations in p-Pb collisions at root s(NN) = 5.02 TeV using the ALICE detector at the Large Hadron Collider are presented. These correlations are used to separate the production of associated Lambda baryons into three different kinematic regions, namely those produced in the direction of the trigger particle (near side), those produced in the opposite direction (away side), and those whose production is uncorrelated with the jet axis (underlying event). The per-trigger associated Lambda yields in these regions are extracted, along with the near- and away-side azimuthal peak widths, and the results are studied as a function of associated particle pT and event multiplicity. Comparisons with the DPMJET event generator and previous measurements of the phi(1020) meson are also made. The final results indicate that strangeness production in the highest multiplicity p-Pb collisions is enhanced relative to low multiplicity collisions in both the jetlike regions and the underlying event. The production of Lambda relative to charged hadrons is also enhanced in the underlying event when compared to the jetlike regions. Additionally, the results hint that strange quark production in the away-side of the jet is modified by soft interactions with the underlying event.

PHYSICAL REVIEW C 111[1], 015201, 2025. DOI: 10.1103/PhysRevC.111.015201

[P088-2025] "Latin American Strategy Forum for Research Infrastructure (III LASF4RI Contribution)"

Aguilar, A. C.*; Bashir, A.; Cobos-Martinez, J. J.; et al.

The Electron-Ion Collider (EIC), a next generation electron--hadron and electron-nuclei scattering facility, will be built at Brookhaven National Laboratory. The wealth of new data will shape research in hadron physics, from nonperturbative QCD techniques to perturbative QCD improvements and global QCD analyses, for the decades to come. With the present proposal, Latin America based physicists, whose expertise lies on the theory and phenomenology side, make the case for the past and future efforts of a growing community, working hand-in-hand towards developing theoretical tools and predictions to analyze, interpret, and optimize the results that will be obtained at the EIC, unveiling the role of the glue that binds us all. This effort is along the lines of various initiatives taken in the USA and supported by colleagues worldwide, such as the ones by the EIC User Group which were highlighted during the Snowmass Process and the Particle Physics Project Prioritization Panel (P5).

BRAZILIAN JOURNAL OF PHYSICS 55[4], 145, 2025. DOI: 10.1007/s13538-025-01778-x

[P089-2025] "Lead iodide thin films deposited by sputtering: The effect of deposition temperature on the optical and structural properties"

Silva Filho, J. M. C. da*; Borrero, N. F. V.*; Morais, A. de; Freitas, J. N. de; **Marques, F. das C.***

Lead iodide (PbI2) is a 2D layered semiconductor used in several electronic applications, such as solar cells, Xray, and gamma--ray detectors. Most of its properties have been reported for monocrystals or polycrystalline thick films used in high-energy photon detectors. As for thin films used in other optoelectronic devices, the reported properties are limited to the conditions adopted in manufacturing the devices. Furthermore, very little is known about the properties of films deposited by sputtering. Here, we investigate the optical and structural properties of PbI2 thin films deposited by rf-sputtering a PbI2 target.

The deposition temperature significantly influences the film's properties, as determined by X-ray, scanning electron microscopy (SEM), atomic force microscopy (AFM), UV-vis, and Raman spectroscopy. A common characteristic at all temperatures was forming metallic lead (Pb) segregated in the surface of films, with concentration depending on the deposition temperature. These lead clusters were successfully converted into PbI2 using an iodination process, allowing the synthesis of pure PbI2 films without lead segregation. The activation energy for the reaction between Pb clusters and iodine vapor was determined by adopting the Arrhenius equation. It was also observed that converting PbI2 film into perovskite through the two-step process, by immersion of the PbI2 film into methylammonium iodide solution, transforms the segregated lead into perovskite. The sputtering technique allows the deposition of uniform films over large areas compatible with roll-to-roll processes, which are desired to produce large-area detectors and perovskite solar cells.

NEXT ENERGY 6, 100192, 2025. DOI: 10.1016/j.nxener.2024.100192

[P090-2025] "Machine learning-based analysis of electronic properties as predictors of anticholinesterase activity in chalcone derivatives"

Buzelli, T.; **Ipaves, B.***; Gollino, F.; Almeida, W. P.; **Galvao, D. S.***; Autreto, P. A. da S.

In this study, we investigated the correlation between the electronic properties of anticholinesterase compounds and their biological activity. While this correlation has been effectively explored in previous studies, we employed a more advanced approach: machine learning. We analyzed a set of 22 molecules sharing a similar chalcone skeleton, categorizing them into two groups based on their IC50 indices: high and low activity. Using the open-source software Orca, we calculated the geometries and electronic structures of these molecules. Over a hundred parameters were extracted, including Mulliken and Lowdin electronic populations, molecular orbital energies, and Mayer's free valences, forming the foundation for machine learning features. Through our analysis, we developed models capable of distinguishing between the two groups. Notably, the most informative descriptor relied solely on electronic populations and orbital energies. Identifying computationally relevant properties for biological activity enhances drug development efficiency, saving time and resources.

COMPUTATIONAL AND THEORETICAL CHEMISTRY 1249, 115268, 2025. DOI: 10.1016/j.comptc.2025.115268

[P091-2025] "Magnetic properties and dipolar interactions of Fe3O4 nanoparticle clusters produced by bottom-up self--assembly"

Fabris, F.*; Almeida, A. A.*; Ribeiro, P. R. T.*; Pirota, K. R.*; Muraca, D.*

Magnetic nanoparticles (MNPs) exhibit unique magnetic behaviors that make them highly applicable in various fields such as biomedical technology, energy, and sensing. This study investigates the magnetic properties and dipolar interactions of Fe3O4 nanoparticle clusters with different average sizes (27.4 nm, 79.2 nm, and 112.9 nm) produced by an emulsion-based bottom-up self-assembly process. The MNPs, with an individual size of 9.8 nm, were organized into clusters, and their collective magnetic properties were explored using detailed DC and AC magnetic studies. We applied a phenomenological mean--field model to describe the magnetic behavior of the clusters, including an increase in blocking temperature, energy barriers, and relaxation dynamics as a function of cluster size. The results indicate a significant influence of dipolar interactions on the energy barriers and magnetic moment dynamics, with larger clusters exhibiting stronger dipolar fields. Our findings provide insights into the interaction between nanoparticle arrangement and magnetic properties, which offers potential for the development of novel magnetic materials for advanced applications.

JOURNAL OF MATERIALS CHEMISTRY C 13[19], p. 9756-9767, 2025. DOI: 10.1039/d5tc00022j

[P092-2025] "Magnetocaloric Effect and Critical Behavior across the Second-Order Ferromagnetic-Paramagnetic Phase Transition of a NdSmNiMnO6 Double Perovskite"

Attah-Baah, J. M.; Silva Junior, R. S.; Santos, C.; **Carvalho, M. H.*;** Ferreira, N. S.

A key challenge remains to improve or discover magnetic solids with optimal magnetocaloric effect (MCE) performance, providing a promising and environmentally friendly cooling technology. Herein, we report the crystal structure, magnetocaloric effect, and critical behavior of double perovskite NdSmNiMnO6 synthesized by the modified sol-gel process. X-ray diffraction structural investigation reveals that NdSmNiMnO6 crystallizes in the monoclinic P2 1/n (14) space group. The magnetocaloric analysis unveils a maximum magnetic entropy change of -Delta S M max = 2.38 J kg-1 K-1 (at 0-7 T) near the ferromagnetic to paramagnetic second-order phase transition at 180 K. Furthermore, the estimated relative cooling power value increases from similar to 25 to similar to 182 kg-1 K-1 when the applied field changes up to 0-7 T, suggesting a promisor magnetic refrigerant material. The critical behavior investigated by techniques such as the modified Arrott plot, the Kouvel-Fisher method, and the critical isotherm analysis reliably yields critical exponents beta = 0.469, gamma = 0.978, and delta = 3.09, in agreement with the scaling hypothesis. Lastly, the renormalization group theory analysis revealed a magnetic interaction distance decaying as J(r) proportional to r -4.63, which is between the three-dimensional (3D) Heisenberg and the mean-field models, suggesting that the critical behavior of NdSmNiMnO6 can be attributed to the competition between long- and short-range magnetic interactions.

ACS OMEGA 10[18], p.18973-18985, 2025. DOI: 10.1021/acsomega.5c00940

[P093-2025] "Measurement of multidifferential cross sections for dijet production in proton-proton collisions at √s=13TeV"

Hayrapetyan, A.; Tumasyan, A.; Adam, W.; **Chinellato, J. A.*;** et al.
CMS Collaboration

A measurement of the dijet production cross section is reported based on proton-proton collision data collected in 2016 at root s = 13 TeV by the CMS experiment at the CERN LHC, corresponding to an integrated luminosity of up to 36.3 fb(-1). Jets are reconstructed with the anti-k(T) algorithm for distance parameters of R = 0.4 and 0.8. Cross sections are measured double-differentially (2D) as a function of the largest absolute rapidity vertical bar y vertical bar(max) of the two jets with the highest transverse momenta p(T) and their invariant mass m(1,2), and triple-differentially (3D) as a function of the rapidity separation y*, the total boost y(b), and either m(1,2) or the average p(T) of the two jets. The cross sections are unfolded to correct for detector effects and are compared with fixed-order calculations derived at next-to-next-to-leading order in perturbative quantum chromodynamics. The impact of the measurements on the parton distribution functions and the strong coupling constant at the mass of the Z boson is investigated, yielding a value of alpha(S)(m(Z)) = 0.1179 +/- 0.0019.

EUROPEAN PHYSICAL JOURNAL C 85[1], 72, 2025. DOI: 10.1140/epjc/s10052-024-13606-8

[P094-2025] "Nanophotonics of mid-infrared plasmon-polaritons at interfaces between metals and two-dimensional crystals"

Feres, F. H.; Barcelos, I. D.; Bahamon, D. A.; Levandoski, J. E.; Mancini, A.; Santos, T. M. dos; **Mayer, R. A.***; Camargo, D. H. S.; Bufon, C. C. B.; Cernescu, A.; Maier, S. A.; Freitas, R. de O.; Maia, F. C. B.

The optical response of metal/dielectric interfaces is largely influenced by surface plasmon-polariton (SPP) modes. In the mid-infrared (IR) range, SPPs can probe the inner physicochemical properties of metal/dielectric systems, including interfaces with mid-IR polaritonic 2D crystals. Using advanced nanoscopy techniques, we characterize mid-IR SPP modes at air/gold and hexagonal boron nitride (hBN) 2D crystal/gold interfaces via synchrotron infrared nanospectroscopy (SINS) and scattering-scanning near-field optical microscopy (s-SNOM) imaging. SPPs in these systems show micrometer-sized wavelengths and propagation lengths over 20 micrometers at room temperature. In hBN/Au, both SPPs and hyperbolic phonon polaritons (HPhPs) coexist, creating SPP-HPhP wave superposition. The experimental momentum and damping of the SPP waves are determined from the s-SNOM imaging and the SINS spatio-spectral linescan. Thereby, we retrieve the experimental frequency-momentum dispersion relation, presenting excellent agreement with theory. Furthermore, we characterize an anti-crossing of the SPP dispersion near the in-plane transverse optical phonon frequency of hBN, indicating that SPP modes and phonon form a coupled system interacting in the strong coupling regime. Such an interaction of SPPs with phonons can be further explored to enhance the sensibility of mid-IR nanospectroscopy techniques.

NANOSCALE 17[21], p. 13229-13237, 2025. DOI: 10.1039/d4nr04543b

[P095-2025] "Non-classicality and non-adiabaticity in a single trapped ion"

Avalos, C. F. P.*; Oliveira, M. C. de*

Trapped ion systems present non-classical characteristics such as squeezed states that show a quantum advantage in quantum sensing, quantum information processing and quantum thermodynamics. We analyze the non-classical characteristics of a system described by a single ion trapped by a periodic potential field. Within the regime of non-adiabatic manipulation of the potential field, the dynamics of motion of the center of mass of the ion can be described by a dimensionless parameter called the non-adiabatic parameter Q & lowast;. This parameter allows us to distinguish the classical and non-classical characteristics of the system. Using the equations of motion of observables in the Heisenberg picture, we propose an analysis of the unitary time evolution operator and discuss the squeezing behavior in the state of motion of the ion. The results shown can serve as a basis to discuss the presence of squeezing as a resource in quantum thermodynamics in the non-adiabatic regime in actual achievable experimental limitations.

NEW JOURNAL OF PHYSICS 27[2], 023028, 2025. DOI: 10.1088/1367-2630/adb646

[P096-2025] "Nonreciprocal multipartite entanglement induced by Kerr nonlinearity"

Ahmed, R.; Ali, H.; Shehzad, A.; Singh, S. K.; **Sohail, A.*; Oliveira, M. C. de***

We present a theoretical scheme for the generation of nonreciprocal multipartite entanglement in a two-mode cavity magnomechanical system, consisting of two cross-microwave cavities having a yttrium-iron-garnet (YIG) sphere, which is coupled through magnetic dipole interaction. Our results show that the self-Kerr effect of magnon (which depends on the intensity of the magnons) can significantly enhance multipartite entanglement, which turns out to be nonreciprocal when the magnetic field is tuned along different crystallographic axes. This is due to the frequency shift on the magnons (YIG sphere), which depends upon the magnetic field's direction. Interestingly, the degree of nonreciprocity of bipartite entanglements depends upon a careful optimal choice of system parameters like normalized cavity detunings, bipartite nonlinear index Delta EK, self-Kerr coefficient, and effective magnomechanical coupling rate G. In addition to bipartite entanglement, we also present the idea of a bidirectional contrast ratio, which quantifies the nonreciprocity in tripartite entanglements. Our present theoretical proposal for nonreciprocity in multipartite entanglement may find applications in diverse engineering nonreciprocal devices. Furthermore, the current scheme might enhance the functionality of magnonic devices, and improve sensing capabilities.

QUANTUM INFORMATION PROCESSING 24[5], 137, 2025. DOI: 10.1007/s11128-025-04757-y

[P097-2025] "Numerical Investigation of the Interaction of Tubular Hollow-Core Fibers and Flexural Acoustic Waves"

Silva, R. E. da; **Osorio, J. H.*; Rodrigues, G. L.***; Webb, D. J.; Gerome, F.; Benabid, F.; **Cordeiro, C. M. B.***; Franco, M. A. R.

The modulation efficiency of a tubular-lattice hollow-core fiber (HCF) employing flexural acoustic waves is investigated in detail for the first time. The main acousto-optic properties of the HCF are evaluated, using 2D and 3D models based on the finite element method. The induced coupling of the fundamental and first higher-order modes is simulated from 743 to 1355 nm. The most relevant acoustic (amplitude, period, strain, energy) and optical (effective index, beat length, birefringence, coupling coefficient) parameters are analyzed. The simulations are compared to experimental results and indicate higher modulation performance in HCFs compared to standard optical fibers. In addition, useful insights into the design and fabrication of all-fiber acousto-optic devices based on HCFs are provided, enabling potential application in tunable spectral filters and mode-locked fiber lasers.

JOURNAL OF LIGHTWAVE TECHNOLOGY 43[11], p. 5423-5429, 2025. DOI: 10.1109/JLT.2025.3549948

[P098-2025] "Optical Memory in a MoSe2/Clinochlore Device"

Ames, A.; Sousa, F. B.; Souza, G. A. D.; Oliveira, R. de; Silva, I. R. F.; **Rodrigues, G. L.***; Watanabe, K.; Taniguchi, T.; Marques, G. E.; Barcelos, I. D.; Cadore, A. R.; Lopez-Richard, V.; Teodoro, M. D.

Two-dimensional heterostructures have been crucial in advancing optoelectronic devices utilizing van der Waals materials. Semiconducting transition-metal dichalcogenide monolayers, known for their unique optical properties, offer extensive possibilities for light-emitting devices. Recently, a memory-driven optical device, termed a Mem-emitter, was proposed by using these monolayers atop dielectric substrates.The successful realization of such devices heavily depends on the selection of the optimal substrate. Here, we report a pronounced memory effect in a MoSe2/clinochlore device, evidenced by an electric hysteresis in the intensity and energy of MoSe2 monolayer emissions.

This demonstrates both population- and transition-rate-driven Mem-emitter abilities. Our theoretical approach correlates these memory effects with internal state variables of the substrate, emphasizing that a clinochlore-layered structure is crucial for a robust and rich memory response. This work introduces a novel two-dimensional device with promising applications in memory functionalities, highlighting the importance of alternate insulators in the fabrication of van der Waals heterostructures.

ACS APPLIED MATERIALS & INTERFACES 17[8], p. 12818-12826, 2025. DOI: 10.1021/acsami.4c19337

[P099-2025] "Particle production as a function of charged--particle flattenicity in pp collisions at √sp=13TeV"

Acharya, S.; Adamova, D.; Agarwal, A.; **Chinellato, D. D.*; Guardiano, G. G.*; Liveraro, G. S. S.*; Takahashi, J.***; et al. ALICE Collaboration

This paper reports the first measurement of the transverse momentum (p(T)) spectra of primary charged pions, kaons, (anti)protons, and unidentified particles as a function of the charged-particle flattenicity in pp collisions at root s = 13 TeV. Flattenicity is a novel event shape observable that is measured in the pseudorapidity intervals covered by the V0 detector, 2.8 < eta < 5.1 and -3.7 < eta < -1.7. According to QCD-inspired phenomenological models, it shows sensitivity to multiparton interactions and is less affected by biases toward larger pT due to local multiplicity fluctuations in the V0 acceptance than multiplicity. The analysis is performed in minimum-bias (MB) as well as in high-multiplicity events up to p(T) = 20 GeV/c. The event selection requires at least one charged particle produced in the pseudorapidity interval |eta| < 1. The measured p(T) distributions, average p(T), kaon-to--pion and proton-to-pion particle ratios, presented in this paper, are compared to model calculations using PYTHIA 8 based on color strings and EPOS LHC. The modification of the p(T)-spectral shapes in low-flattenicity events that have large event activity with respect to those measured in MB events develops a pronounced peak at intermediate p(T) (2 < p(T) < 8 GeV/c), and approaches the vicinity of unity at higher p(T). The results are qualitatively described by PYTHIA, and they show different behavior than those measured as a function of chargedparticle multiplicity based on the V0M estimator.

PHYSICAL REVIEW D 111[1], 2025. DOI: 10.1103/PhysRevD.111.012010

[P100-2025] "Phase-space approach to cavity field dynamics in a squeezed thermal reservoir"

Mattos, E. P.*; Vidiella-Barranco, A.*

Quantum systems, such as a single-mode cavity field coupled to a thermal bath, typically experience destructive effects due to interactions with their noisy environment. When the bath combines both thermal fluctuations and a nonclassical feature like quadrature squeezing, forming a squeezed thermal reservoir, the system's behavior can change substantially. In this work, we study the evolution of the cavity field in this generalized environment using an alternative phase-space approach based on the Glauber-Sudarshan P-function. We derive a compact analytical expression for the time-dependent P-function for arbitrary initial cavity field states and demonstrate its utility through specific examples.Additionally, we obtain analytical expressions, as a function of time, for some statistical properties of the cavity field, as well as for the nonclassical depth, am, a nonclassicality measure calculated directly from the P-function.

ANNALS OF PHYSICS 479, 170055, 2025. DOI: 10.1016/j.aop.2025.170055

[P101-2025] "Phosphoferrene for Mancozeb detection: A natural 2D phosphate mineral enhancing pesticide sensing"

Slathia, S.Santos, A. B.; Costin, G.; Sarkar, S.; Glavin, N. R.; Roy, A. K.; **Galvao, D. S.***; Woellner, C. F.; Tiwary, C. S.

The fungicide mancozeb is widely used to protect crops and fruits from pests and boost their yields. Nevertheless, there are significant health and environmental hazards associated with these chemical residues. In this study, we used phosphoferrene, a naturally occurring layered 2D phosphate mineral, to detect mancozeb. The interaction mechanism between MNZ molecules and the phosphoferrene surface was primarily characterized by physical adsorption, with limited possibilities for weak interaction occurring between the sulfur atoms of MNZ and the oxygen atoms of phosphoferrene, as evidenced by FTIR and DFT analyses. A dual detection approach was utilized, incorporating UV-vis spectroscopy in the linear range of 0.185 mM to 1.85 mu M with a LOD of 0.85 mu M in conjunction with an electrochemical method, facilitating real-time monitoring of mancozeb. The developed sensing electrode exhibited a linear range spanning from 0.185 mM to 0.92 mu M, with a limit of detection approximated at 0.085 mu M. This study can contribute to the monitoring of permissible limits of mancozeb in agricultural fields, thereby minimizing the risk of overdosage. Additionally, it provides valuable insights for researchers seeking pathways for the degradation of the mancozeb fungicide and developing more safer alternatives.

JOURNAL OF ENVIRONMENTAL CHEMICAL ENGINEERING 13[3], 116614, 2025. DOI: 10.1016/j.jece.2025.116614

[P102-2025] "PoWER: a new concept for DUNE Phase 2 FD PDS"

Steklain, A.; **Segreto, E.*; Machado, A.***; Adames, M.; Hirsch, L.; Di Capua, F.; Canci, N.; **Frandini, H.***

We propose a novel concept for the future modules of the DUNE Phase 2 Far Detector Photodetection System, namely the Polymer Wavelength shifter and Enhanced Reflection - PoWER. In this concept, the field cage of the LArTPC is entirely covered with polymeric wavelength shifting foils (PolyEthylene Naphthalate - PEN) to convert the liquid argon scintillation light from VUV to visible, and an Enhanced Specular Reflector (ESR) is installed on the membrane aiming to increase the number of reflections and consequently the detection probability. In addition, we use Light Detection Units (LDUs), which are a combination of standard and VUV-sensitive SiPM that can be used as an active veto for events occurring outside the field cage. We present a preliminary study using a Monte Carlo simulation, including a Light Map for photons generated inside the field cage and a demonstration of the active veto.

JOURNAL OF INSTRUMENTATION 20[4], C04008, 2025. DOI: 10.1088/1748-0221/20/04/C04008

[P103-2025] "Predictions for dimuon production in high--energy neutrino-proton collisions using the color dipole model"

Ternes, C.*; Fagundes, D. A.; Huayra, E.; Oliveira, E. G. de

Interactions of high-energy neutrinos with matter can be studied through the angular separation observed in dimuon production, an observable particularly sensitive to the transverse momentum dynamics of partons. In this work, we develop a Monte Carlo event generator based on the color dipole model, interfaced with Pythia8 for parton showering and hadronization simulations, to predict dimuon production cross sections in neutrino-proton collisions at energies relevant to IceCube and future detectors.

The color dipole formalism generates larger transverse momentum compared to standard Pythia predictions, enhancing the yield of angularly separated high-energy muons.

JOURNAL OF HIGH ENERGY PHYSICS [5], 25, 2025. DOI: 10.1007/JHEP05(2025)025

[P104-2025] "Probing a low-mass Z' gauge boson at IceCube and prospects for IceCube-Gen2"

Francener, R.*; Gonçalves, V. P.; **Gratieri, D. R.***

In this work, we investigate the impact of the L L, - L Lz model, which predicts a new massive gauge boson Z Z' on astrophysical neutrino events at the IceCube Observatory. This new gauge boson couples with leptons from the second and third families and would break the power law of the astrophysical neutrino flux due to the interaction of this flux with the cosmic neutrino background. We derive the sensitivity of IceCube to this model considering the high-energy start events data from 12 years of observation by assuming different assumptions for the redshift distributions of astrophysical neutrino sources, mass ordering, and sum of neutrino masses. Our results indicate that the current IceCube data are able to probe small coupling and masses on the order of some few MeV, with the covered parameter space being larger if a distribution of neutrino sources is described by the star formation rate model. In addition, we demonstrate that IceCube--Gen2 will cover a large region of the parameter space and will allow us to improve our understanding of the L L, - L Lz model.

PHYSICAL REVIEW D 111[9], 095005, 2025. DOI: 10.1103/PhysRevD.111.095005

[P105-2025] "Probing n-Type Conduction in Eumelanin Using Organic Electrochemical Transistors"

Nozella, N. L.; Paulin, J. V.; Nogueira, G. L.; Guerra, N. B.; **Oliveira, R. F. de***; Graeff, C. F. O.

Sustainability demands innovative materials and technologies to address environmental and societal needs. In this context, natural biomaterials are gaining significant attention, with eumelanin (EuM) standing out due to its biocompatibility, abundance, and distinct electronic properties. However, the conducting nature of EuM and the main carrier involved in the charge transport have been the subject of a long-standing and inconclusive debate. This work contributes to this discussion by presenting the observation of n-type conduction in EuM films employed as channel material in organic electrochemical transistors (OECTs). The device current is modulated based on strong ionic electronic coupling between electrolyte cations and the pi electron system of EuM's indole units, resulting in charge mobility of mu OECT = 0.019 +/- 0.016 cm2 V-1 s-1. Our findings provide an innovative contribution to the ongoing debate on the semiconducting properties of EuM and demonstrate a novel electronic device, highlighting the remarkable potential of EuM for sustainable electronics.

ACS APPLIED ELECTRONIC MATERIALS 7[8], p. 3176-3181, 2025. DOI: 10.1021/acsaelm.5c00293

[P106-2025] "Probing Strangeness Hadronization with Event-by-Event Production of Multistrange Hadrons"

Acharya, S.; Adamova, D.; Agarwal, A.; **Chinellato, D. D.*; Guardiano, G. G.*; Liveraro, G. S. S.*; Takahashi, J.***; et al.
ALICE Collaboration

This Letter presents the first measurement of event-by--event fluctuations of the net number (difference between the particle and antiparticle multiplicities) of multistrange hadrons Xi(-) and (Xi) over bar (+) and its correlation with the net-kaon number using the data collected by the ALICE Collaboration in pp, p-Pb, and Pb-Pb collisions at a center--of-mass energy per nucleon pair root s(NN) = 5.02 TeV. The statistical hadronization model with a correlation over three units of rapidity between hadrons having the same and opposite strangeness content successfully describes the results. On the other hand, string-fragmentation models that mainly correlate strange hadrons with opposite strange quark content over a small rapidity range fail to describe the data.

PHYSICAL REVIEW LETTERS 134[2], 022303, 2025. DOI: 10.1103/PhysRevLett.134.022303

[P107-2025] "Pseudorapidity distributions of charged hadrons in lead-lead collisions at √SNN=5.36 TeV"

Hayrapetyan, A.; Tumasyan, A.; Adam, W.; **Chinellato, J. A.***; et al.
CMS Collaboration

The pseudorapidity (eta) distributions of charged hadrons are measured using data collected at the highest ever nucleon--nucleon center-of-mass energy of root s(NN) = 5.36 TeV for collisions of lead-lead ions. The data were recorded by the CMS experiment at the LHC in 2022 and correspond to an integrated luminosity of 0.30 +/- 0.03 mu b(-1). Using the CMS silicon pixel detector, the yields of primary charged hadrons produced in the range |eta| < 2.6 are reported. The evolution of the midrapidity particle density as a function of collision centrality is also reported. In the 5% most central collisions, the charged--hadron eta density in the range |eta| < 0.5 is found to be 2032 +/- 91 (syst), with negligible statistical uncertainty. This result is consistent with an extrapolation from nucleus-nucleus collision data at lower center-of-mass energies. Comparisons are made to various Monte Carlo event generators and to previous measurements of lead-lead and xenon-xenon collisions at similar collision energies. These new data detail the dependence of particle production on the collision energy, initial collision geometry, and the size of the colliding nuclei.

PHYSICS LETTERS B 861, 139279, 2025. DOI: 10.1016/j.physletb.2025.139279

[P108-2025] "Search for a heavy resonance decaying into a Z and a Higgs boson in events with an energetic jet and two electrons, two muons, or missing transverse momentum in proton-proton collisions at √s=13 TeV"

Hayrapetyan, A.; Tumasyan, A.; Adam, W.; **Chinellato, J. A.***; et al.
CMS Collaboration

A search is presented for a heavy resonance decaying into a Z boson and a Higgs (H) boson. The analysis is based on data from proton-proton collisions at a centre-of-mass energy of 13TeV corresponding to an integrated luminosity of 138 fb(-1), recorded with the CMS experiment in the years 2016-2018.Resonance masses between 1.4 and 5TeV are considered, resulting in large transverse momenta of the Z and H bosons. Final states that result from Z boson decays to pairs of electrons, muons, or neutrinos are considered. The H boson is reconstructed as a single large-radius jet, recoiling against the Z boson. Machine-learning flavour-tagging techniques are employed to identify decays of a Lorentz--boosted H boson into pairs of charm or bottom quarks, or into four quarks via the intermediate H -> WW* and ZZ* decays.

The analysis targets H boson decays that were not generally included in previous searches using the H -> b (b) over bar channel. Compared with previous analyses, the sensitivity for high resonance masses is improved significantly in the channel where at most one b quark is tagged.

JOURNAL OF HIGH ENERGY PHYSICS [2], 089, 2025. DOI: 10.1007/JHEP02(2025)089

[P109-2025] "Search for charged-lepton flavor violation in the production and decay of top quarks using trilepton final states in proton-proton collisions at √s=13 TeV"

Hayrapetyan, A.; Tumasyan, A.; Adam, W.; **Chinellato, J. A.***; et al.
CMS Collaboration

A search is performed for charged-lepton flavor violating processes in top quark (t) production and decay. The data were collected by the CMS experiment from proton-proton collisions at a center-of-mass energy of 13 TeV and correspond to an integrated luminosity of 138 fb(-1). The selected events are required to contain one opposite-sign electron-muon pair, a third charged lepton (electron or muon), and at least one jet of which no more than one is associated with a bottom quark. Boosted decision trees are used to distinguish signal from background, exploiting differences in the kinematics of the final states particles. The data are consistent with the standard model expectation. Upper limits at 95% confidence level are placed in the context of effective field theory on the Wilson coefficients, which range between 0.024-0.424 TeV-2 depending on the flavor of the associated light quark and the Lorentz structure of the interaction. These limits are converted to upper limits on branching fractions involving up (charm) quarks, t -> e mu u (t -> e mu c), of 0.032(0.498) x 10(-6), 0.022(0.369) x 10(-6), and 0.012(0.216) x 10(-6) for tensorlike, vectorlike, and scalarlike interactions, respectively.

PHYSICAL REVIEW D 111[1], 012009, 2025. DOI: 10.1103/PhysRevD.111.012009

[P110-2025] "Search for long-lived heavy neutral leptons in proton-proton collision events with a lepton-jet pair associated with a secondary vertex at √s=13 TeV"

Hayrapetyan, A.; Tumasyan, A.; Adam, W.; **Chinellato, J. A.***; et al.
CMS Collaboration

A search for long-lived heavy neutral leptons (HNLs) using proton-proton collision data corresponding to an integrated luminosity of 138 fb(-1) collected at root s = 13TeV with the CMS detector at the CERN LHC is presented. Events are selected with a charged lepton originating from the primary vertex associated with the proton-proton interaction, as well as a second charged lepton and a hadronic jet associated with a secondary vertex that corresponds to the semileptonic decay of a long-lived HNL. No excess of events above the standard model expectation is observed. Exclusion limits at 95% confidence level are evaluated for HNLs that mix with electron and/or muon neutrinos. Limits are presented in the mass range of 1-16.5 GeV, with excluded square mixing parameter values reaching as low as 2 x 10(-7). For masses above 11 GeV, the presented limits exceed all previous results in the semileptonic decay channel, and for some of the considered scenarios are the strongest to date.

JOURNAL OF HIGH ENERGY PHYSICS [2], 36, 2025. DOI: 10.1007/JHEP02(2025)036

[P111-2025] "Search for pair production of heavy particles decaying to a top quark and a gluon in the lepton plus jets final state in proton-proton collisions at √s=13 TeV"

Hayrapetyan, A.; Tumasyan, A.; **Chinellato, J. A.***; et al.
CMS Collaboration

A search is presented for the pair production of new heavy resonances, each decaying into a top quark (t) or antiquark and a gluon (g). The analysis uses data recorded with the CMS detector from proton-proton collisions at a center-of-mass energy of 13 TeV at the LHC, corresponding to an integrated luminosity of 138 fb(-1). Events with one muon or electron, multiple jets, and missing transverse momentum are selected. After using a deep neural network to enrich the data sample with signal-like events, distributions in the scalar sum of the transverse momenta of all reconstructed objects are analyzed in the search for a signal. No significant deviations from the standardmodel prediction are found. Upper limits at 95% confidence level are set on the product of cross section and branching fraction squared for the pair production of excited top quarks in the t* -> tg decay channel. The upper limits range from 120 to 0.8 fb for a t* with spin-1/2 and from 15 to 1.0 fb for a t* with spin-3/2. These correspond to mass exclusion limits up to 1050 and 1700 GeV for spin-1/2 and spin-3/2 t* particles, respectively. These are the most stringent limits to date on the existence of t* -> tg resonances.

EUROPEAN PHYSICAL JOURNAL C 85[3], 342, 2025. DOI: 10.1140/epjc/s10052-024-13729-y

[P112-2025] "Search for resonant pair production of Higgs bosons in the b(b)over-barb(b)over-bar final state using large-area jets in proton-proton collisions at √s=13 TeV"

Tumasyan, A.; Adam, W.; Andrejkovic, J. W.; **Chinellato, J. A.***; et al.
CMS Collaboration

A search is presented for the resonant production of a pair of standard model-like Higgs bosons using data from proton--proton collisions at a centre-of-mass energy of 13 TeV, collected by the CMS experiment at the CERN LHC in 2016-2018, corresponding to an integrated luminosity of 138 fb(-1). The final state consists of two b quark-antiquark pairs. The search is conducted in the region of phase space where at least one of the pairs is highly Lorentz-boosted and is reconstructed as a single large-area jet. The other pair may be either similarly merged or resolved, the latter reconstructed using two b-tagged jets. The data are found to be consistent with standard model processes and are interpreted as 95% confidence level upper limits on the product of the cross sections and the branching fractions of the spin-0 radion and the spin-2 bulk graviton that arise in warped extradimensional models. The limits set are in the range 9.74-0.29 fb and 4.94-0.19 fb for a narrow radion and a graviton, respectively, with masses between 1 and 3 TeV. For a radion and for a bulk graviton with widths 10% of their masses, the limits are in the range 12.5-0.35 fb and 8.23-0.23 fb, respectively, for the same masses. These limits result in the exclusion of a narrow-width graviton with a mass below 1.2 TeV, and of narrow and 10%-width radions with masses below 2.6, and 2.9 TeV, respectively.

JOURNAL OF HIGH ENERGY PHYSICS [2], 040, 2025. DOI: 10.1007/JHEP02(2025)040

[P113-2025] "Search for the Anomalous Events Detected by ANITA Using the Pierre Auger Observatory"

Abdul Halim, A.; Abreu, P.; Aglietta, M.; **Arbeletche, L. B.*; Chinellato, J. A.*; Dobrigkeit, C.*; Fauth, A. C.*; Payeras, A. M.*; Reginatto Akim, J. V.***; et al.
Pierre Auger Collaboration

A dedicated search for upward-going air showers at zenith angles exceeding 110° and energies E>0.1EeV has been performed using the Fluorescence Detector of the Pierre Auger Observatory. The search is motivated by two "anomalous" radio pulses observed by the ANITA flights I and III that appear inconsistent with the standard model of particle physics. Using simulations of both regular cosmic-ray showers and upward-going events, a selection procedure has been defined to separate potential upward-going candidate events and the corresponding exposure has been calculated in the energy range [0.1-33] EeV. One event has been found in the search period between January 1, 2004, and December 31, 2018, consistent with an expected background of 0.27±0.12 events from misreconstructed cosmic-ray showers. This translates to an upper bound on the integral flux of (7.2±0.2)*10^{-21}cm^{-2}sr^{-1}y^{-1} and (3.6±0.2)*10^{-20}cm^{-2}sr^{-1}y^{-1} for an E^{-1} and E^{-2} spectrum, respectively. An upward-going flux of showers normalized to the ANITA observations is shown to predict over 34 events for an E^{-3} spectrum and over 8.1 events for a conservative E^{-5} spectrum, in strong disagreement with the interpretation of the anomalous events as upward-going showers.

PHYSICAL REVIEW LETTERS 134[12], 121003, 2025. DOI: 10.1103/PhysRevLett.134.121003

[P114-2025] "Semianalytical algorithms to study longitudinal beam instabilities in double rf systems"

Gamelin, A.; Gubaidulin, V.; **Alves, M. B.***; Olsson, T.

Double rf systems are critical for achieving the parameters of fourth-generation light sources. These systems, comprising both main and harmonic rf cavities, relax statistical collective effects but also introduce instabilities, such as Robinson and periodic transient beam loading (PTBL) instabilities. In this paper, we provide semianalytical algorithms designed to predict and analyze these instabilities with improved accuracy and robustness. The algorithms leverage recent advancements in the field, offering a computationally efficient and accurate complement to multibunch tracking simulations. Using the SOLEIL II project as a case study, we demonstrate how these algorithms can optimize rf cavity parameters in high-dimensional parameter spaces, thereby maximizing the Touschek lifetime. An open-source Python package, ALBuMS (Algorithms for Longitudinal Multibunch Beam Stability), is provided as an accessible tool for double rf system stability analysis.

PHYSICAL REVIEW ACCELERATORS AND BEAMS 28[5], 054401, 2025. DOI: 10.1103/PhysRevAccelBeams.28.054401

[P115-2025] "Shape-Induced Enhanced Raman Scattering (SIERS) Platforms Modified with Gold Nanorods for Ultratiluted Atrazine Pesticide Detection"

Ferreira, M. G.; Barros, A. de; **Shimizu, F. M.***; Sigoli, F. A.; Bufon, C. C.; Mazali, I. O.

Herein, we explored the shape-induced enhanced Raman scattering (SIERS) effect to detect Atrazine pesticides in different concentrations (1.6 x 10-8-1.6 x 10-20 mol L-1). For this, the performance of the SIERS effect compared to the conventional Raman signal was evaluated using a silicon substrate with a V-shaped (Si-V) microchannel and a flat silicon substrate (flat Si). Experimental data free of metallic nanostructure show that the SIERS effect increases up to a 7-fold signal for the Atrazine molecule compared to the conventional Raman signal. Combining SIERS and surface-enhanced Raman scattering (SERS) effects (SIERS@SERS) using metallic nanostructures is the key feature used to achieve lower limit detection of the target molecule. The performance of SIERS@SERS was evaluated by using gold nanorods (AuNRs) metallic structure deposited onto Si-V and flat Si for the detection of Atrazine in different concentrations (1.6 x 10-8-1.6 x 10-20 mol L-1). The geometric design of V-shaped microchannels also enables a "trap" for the molecule confinement and builds up an excellent electromagnetic field distribution by AuNR aggregates. The AuNRs aggregation is also favored by incubating a AuNRs colloidal suspension mixed with Atrazine using different solvents (water and methanol). In this sense, the results reveal that the solvent plays an important role in the signal intensity as well as spectra definition and band identification. The IDMAP statistical projection reveals good data discrimination with a silhouette coefficient of 0.64 for Si-V substrate (1.6 x 10-8-1.6 x 10-20 mol L-1) against 0.51 for flat Si (1.6 x 10-8-1.6 x 10-16 mol L-1), indicating that the SIERS@SERS effect provides more sensitivity for the sensor. The Si-V platforms are a robust option for commercial sensors, since they can be reusable with or without plasmonic nanostructures.

ACS APPLIED NANO MATERIALS 8[20], p. 10287-10296, 2025. DOI: 10.1021/acsanm.4c07289

[P116-2025] "Skyrmionium dynamics and stability on one dimensional anisotropy patterns"

Souza, J. C. B.; **Vizarim, N. P.***; Reichhardt, C. J. O.; Reichhardt, C.; Venegas, P. A.

We examine a skyrmionium driven over a periodic anisotropy pattern, which consists of disorder free regions and disordered regions. For small defect densities, the skyrmionium flows for an extended range of currents, and there is a critical current above which it transforms into a skyrmion. For increased amounts of quenched disorder, the current needed for the skyrmionium to transform into a skyrmion decreases, and there is a critical disorder density above which a moving skyrmionium is not stable. In the moving state, the skyrmionium to skyrmion transformation leads to a drop in the velocity and the onset of a finite skyrmion Hall angle. We also find a reentrance effect in which the pinned skyrmionium transforms into a skyrmion just above depinning, restabilizes into skyrmionium at larger drives, and becomes unstable again at large currents. We also show that adding a transverse shaking drive can increase the lifetime of a moving skyrmionium by reducing the effect of the pinning in the direction of the drive.

JOURNAL OF PHYSICS-CONDENSED MATTER 37[19], 195802, 2025. DOI: 10.1088/1361-648X/adc648

[P117-2025] "Spin-orbital Kitaev model: From kagome spin ice to classical fractons"

Fontana, W. B.; Oliviero, F. G.; Pereira, R. G.; **Natori, W. M. H.***

We study an exactly solvable spin-orbital model that can be regarded as a classical analog of the celebrated Kitaev honeycomb model and describes interactions between Rydberg atoms on the ruby lattice. We leverage its local and nonlocal symmetries to determine the exact partition function and the static structure factor. A mapping between S = 3/2 models on the honeycomb lattice and kagome spin Hamiltonians allows us to interpret the thermodynamic properties in terms of a classical kagome spin ice. Partially lifting the symmetries associated with line operators, we obtain a model characterized by immobile excitations, called classical fractons, and a ground-state degeneracy that increases exponentially with the length of the system. We formulate a continuum theory that reveals the underlying gauge structure and conserved charges. Extensions of our theory to other lattices and higher-spin systems are suggested.

PHYSICAL REVIEW B 111[19], 195112, 2025. DOI: 10.1103/PhysRevB.111.195112

[P118-2025] "Study of WH production through vector boson scattering and extraction of the relative sign of the W and Z couplings to the Higgs boson in proton-proton collisions at √S=13 Te"

Hayrapetyan, A.; Tumasyan, A.; Adam, W.; **Chinellato, J. A.*;** et al.
CMS Collaboration

A search for the production of a W boson and a Higgs boson through vector boson scattering (VBS) is presented, using CMS data from proton-proton collisions at root s = 13 TeV collected from 2016 to 2018. The integrated luminosity of the data sample is 138 fb(-1). Selected events must be consistent with the presence of two jets originating from VBS, the leptonic decay of the W boson to an electron or muon, possibly also through an intermediate tau lepton, and a Higgs boson decaying into a pair of b quarks, reconstructed as either a single merged jet or two resolved jets. A measurement of the process as predicted by the standard model (SM) is performed alongside a study of beyond-the-SM (BSM) scenarios. The SM analysis sets an observed (expected) 95% confidence level upper limit of 14.3 (9.9) on the ratio of the measured VBS WH cross section to that expected by the SM. The BSM analysis, conducted within the so-called kappa framework, excludes all scenarios with lambda(WZ) < 0 that are consistent with current measurements, where lambda(WZ) = kappa(W)/kappa(Z) and kappa W and kappa(Z) are the HWW and HZZ coupling modfiers, respectively. The significance of the exclusion is beyond 5 standard deviations, and it is consistent with the SM expectation of lambda(WZ) = 1.

PHYSICS LETTERS B 860, 139202, 2025. DOI: 10.1016/j.physletb.2024.139202

[P119-2025] "The CYGNO experiment"

Antonietti, R.; Baracchini, E.; **Saviano, G.***; et al.

The existence of non-luminous matter in the Universe, known as Dark Matter, is a fundamental ingredient of modern cosmological theories. Its nature and characteristics are currently unknown. The CYGNO project, using a directional detector, aims to study events such as Dark Matter interactions in the low mass region O(GeV/c2). The proposed detector is a Time Projection Chamber (TPC), filled with a gas mixture of He:CF4 (60:40) at room temperature and atmospheric pressure. The signal is produced by primary ionization from a few keV nuclear or electron recoil, which is amplified using a triple Gas Electron Multiplier (GEM) stack. During this process, light proportional to the primary electrons is generated. By combining the use of a sCMOS camera and photomultiplier, the signal is acquired allowing for the reconstruction of the energy and direction of the recoils. The R&D phase is concluding with the Long Imaging ModulE (LIME) prototype, a 50 liters TPC. It is currently taking data underground at the Laboratori Nazionali del Gran Sasso (LNGS) to study the performance of the prototype in a low background environment. The latest results on LIME operations in different configurations are shown.

NUOVO CIMENTO C-COLLOQUIA AND COMMUNICATIONS IN PHYSICS 48[3], 95, 2025. DOI: 10.1393/ncc/i2025-25095-0

[P120-2025] "The Distribution of Ultrahigh-energy Cosmic Rays along the Supergalactic Plane Measured at the Pierre Auger Observatory"

Halim, A. A.; Abreu, P.; Aglietta, M.; **Bonneau Arbeletche, L.*; Chinellato, J. A.*; Oliveira Franco, D. de*; Dobrigkeit, C.*; Fauth, A. C.*; Machado Payeras, A.*; Reginatto Akim, J. V.***; et al.
Pierre Auger Collaboration

Ultrahigh-energy cosmic rays are known to be mainly of extragalactic origin, and their propagation is limited by energy losses, so their arrival directions are expected to correlate with the large-scale structure of the local Universe. In this work, we investigate the possible presence of intermediate-scale excesses in the flux of the most energetic cosmic rays from the direction of the supergalactic plane region using events with energies above 20 EeV recorded with the surface detector array of the Pierre Auger Observatory up to 2022 December 31, with a total exposure of 135,000 km2 sr yr. The strongest indication for an excess that we find, with a posttrial significance of 3.1 sigma, is in the Centaurus region, as in our previous reports, and it extends down to lower energies than previously studied. We do not find any strong hints of excesses from any other region of the supergalactic plane at the same angular scale. In particular, our results do not confirm the reports by the Telescope Array Collaboration of excesses from two regions in the Northern Hemisphere at the edge of the field of view of the Pierre Auger Observatory. With a comparable integrated exposure over these regions, our results there are in good agreement with the expectations from an isotropic distribution.

ASTROPHYSICAL JOURNAL 984[2], 123, 2025. DOI: 10.3847/1538-4357/adbdc5

[P121-2025] "The effect of radiation damage on the light yield and uniformity of candidate plastic scintillator tiles for the CMS hadron calorimeter upgrade"

Gevorgyan, A.; Petrosyan, A.; Tumasyan, A.; **Chinellato, J. A.***; et al.
CMS HCAL Collaboration

A study has been performed to understand the effects of radiation damage on various plastic scintillator tiles considered for a possible upgrade of the hadron calorimeter of the CMS detector. Measurements were made with unirradiated tiles and with tiles that had been irradiated in the CMS collision hall to a dose of 44 kGy. Results are presented for the tiles of different shapes in terms of the energy spectrum, efficiency as a function of the position at which each tile was hit, as well as light yield. All the tiles showed a light reduction of up to about 50%. The tiles with the shape currently used in the CMS detector did not see increased non-uniformity of light collection, while a significant disuniformity was observed for the tiles considered as alternatives.

JOURNAL OF INSTRUMENTATION 20[1], P01026, 2025. DOI: 10.1088/1748-0221/20/01/P01026

[P122-2025] "The HIBEAM instrument at the European spallation source"

Santoro, V.; Milstead, D.; Fierlinger, P.; **Kemp, E.***; et al.

The European spallation source (ESS) will be the world's brightest neutron source and will open a new intensity frontier in particle physics. The HIBEAM collaboration aims to exploit the unique potential of the ESS with a dedicated ESS instrument for particle physics which offers world-leading capability in a number of areas. The HIBEAM program includes the first search in thirty years for free neutrons converting to antineutrons and searches for sterile neutrons, ultralight axion dark matter and nonzero neutron electric charge. This paper outlines the capabilities, design, infrastructure, and scientific potential of the HIBEAM program, including its dedicated beamline, neutron optical system, magnetic shielding and control, and detectors for neutrons and antineutrons. Additionally, we discuss the long-term scientific exploitation of HIBEAM, which may include measurements of the neutron electric dipole moment and precision studies of neutron decays.

JOURNAL OF PHYSICS G-NUCLEAR AND PARTICLE PHYSICS 52[4], 040501, 2025. DOI: 10.1088/1361-6471/adc8c2

[P123-2025] "The Pierre Auger Observatory open data"

Halim, A. A.; Abreu, P.; Aglietta, M.; **Bonneau Arbeletche, L.*; Chinellato, J. A.*; Dobrigkeit, C.*; Fauth, A. C.*; Machado Payeras, A.*; Reginatto Akim, J. V.***; et al.
Pierre Auger Collaboration

The Pierre Auger Collaboration has embraced the concept of open access to their research data since its foundation, with the aim of giving access to the widest possible community. A gradual process of release began as early as 2007 when 1% of the cosmic-ray data was made public, along with 100% of the space-weather information. In February 2021, a portal was released containing 10% of cosmic-ray data collected by the Pierre Auger Observatory from 2004 to 2018, during the first phase of operation of the Observatory. The Open Data Portal includes detailed documentation about the detection and reconstruction procedures, analysis codes that can be easily used and modified and, additionally, visualization tools. Since then, the Portal has been updated and extended. In 2023, a catalog of the highest-energy cosmic-ray events examined in depth has been included. A specific section dedicated to educational use has been developed with the expectation that these data will be explored by a wide and diverse community, including professional and citizen scientists, and used for educational and outreach initiatives. This paper describes the context, the spirit, and the technical implementation of the release of data by the largest cosmic-ray detector ever built and anticipates its future developments.

EUROPEAN PHYSICAL JOURNAL C 85[1], 70, 2025. DOI: 10.1140/epjc/s10052-024-13560-5

[P124-2025] "The track-length extension fitting algorithm for energy measurement of interacting particles in liquid argon TPCs and its performance with ProtoDUNE-SP data"

Abud, A. A.; Abi, B.; Acciarri, R.; **Adriano, C.*; Bazetto, M. C. Q.*; Borges Merlo, R.*; Aguiar, R. de*; Almeida, P. de*; Holanda, P. C. de*; Gelli, B.*; Gratieri, D. R.*; Guzzo, M. M.*; Kemp, E.*; Machado, A. A.*; Marques, F. das C.*; Peres, O. L. G.*; Pimentel, V. L.*; Porto Paixao, L. G.*; Segreto, E.***; et al.
DUNE Collaboration

This paper introduces a novel track-length extension fitting algorithm for measuring the kinetic energies of inelastically interacting particles in liquid argon time projection chambers (LArTPCs). The algorithm finds the most probable offset in track length for a track-like object by comparing the measured ionization density as a function of position with a theoretical prediction of the energy loss as a function of the energy, including models of electron recombination and detector response. The algorithm can be used to measure the energies of particles that interact before they stop, such as charged pions that are absorbed by argon nuclei. The algorithm's energy measurement resolutions and fractional biases are presented as functions of particle kinetic energy and number of track hits using samples of stopping secondary charged pions in data collected by the ProtoDUNE-SP detector, and also in a detailed simulation. Additional studies describe the impact of the dE/dx model on energy measurement performance. The method described in this paper to characterize the energy measurement performance can be repeated in any LArTPC experiment using stopping secondary charged pions.

JOURNAL OF INSTRUMENTATION 20[2], P02021, 2025. DOI: 10.1088/1748-0221/20/02/P02021

[P125-2025] "The transition to speciation in the finite genome Derrida-Higgs model: a heuristic solution"

Marquioni, V. M.*; Aguiar, M. A. M. de*

The process of speciation, where an ancestral species divides in two or more new species, involves several geographic, environmental and genetic components that interact in a complex way. Understanding all these elements at once is challenging and simple models can help in unveiling the role of each factor separately. The Derrida-Higgs model describes the evolution of a sexually reproducing population subjected to mutations in a well mixed population. Individuals are characterized by a string with entries +/- 1 representing a haploid genome with biallelic genes. If mating is restricted by genetic similarity, so that only individuals that are sufficiently similar can mate, sympatric speciation, i.e. the emergence of species without geographic isolation, can occur. Only four parameters rule the dynamics: population size N, mutation rate mu, minimum similarity for mating qmin and genome size B. In the limit B ->infinity, speciation occurs if the simple condition qmin>(1 + 4 mu N)(-1) is satisfied. However, this condition fails for finite genomes, and speciation does not occur if the genome size is too small. This indicates the existence of a critical genome size for speciation. In this work, we develop an analytical theory of the distribution of similarities between individuals, a quantity that defines how tight or spread out is the genetic content of the population. This theory is carried out in the absence of mating restrictions, where evolution equations for the mean and variance of the similarity distribution can be derived. We then propose a heuristic description of the speciation transition which allows us to numerically calculate the critical genome size for speciation as a function of the other model parameters. The result is in good agreement with the simulations of the model and may guide further investigations on theoretical conditions for species formation.

JOURNAL OF PHYSICS A-MATHEMATICAL AND THEORETICAL 58[17], 175601, 2025. DOI: 10.1088/1751-8121/adcd33

[P126-2025] "Theoretical models for longitudinal coupled--bunch instabilities driven by harmonic cavities in electron storage rings"

Alves, M. B.*

We present a theoretical framework for analyzing longitudinal coupled-bunch instabilities in double-rf systems with even filling patterns, accounting for potential-well distortion and multiple azimuthal modes. The linearized Vlasov equation is solved in the frequency domain for an arbitrary rf potential to derive the Lebedev equation. We unified different formulations, obtaining results from recent publications as particular cases. Applications to Robinson dipole--quadrupole mode coupling and the periodic transient beam loading (PTBL)/mode-1 instability are presented. Notably, for the first time, theoretical predictions of the mode-1 thresholds show excellent agreement with experimental data. The analysis reveals that the PTBL instability is triggered when coherent focusing is lost for the dipole motion of the coupled-bunch mode-1. We also confirm that this instability is dependent on azimuthal mode interactions and resistant to Landau damping, providing new insights into its mechanism. The methods are implemented in the opensource package pycolleff, offering a useful semianalytical tool for studying instabilities in electron storage rings with harmonic cavities.

PHYSICAL REVIEW ACCELERATORS AND BEAMS 28[3], 034401, 2025. DOI: 10.1103/PhysRevAccelBeams.28.034401

[P127-2025] "Three-Dimensional-Printed Isoniazid Chewable Gels for On-Demand Latent Tuberculosis Treatment in Children"

Moreira, A. de O. E.; Azevedo Neta, L. M. S.; Pietroluongo, M.; Matos, A. P. dos S.; Correa, B. B.; Ortiz, B. H.; Guimaraes, A. de S.; Nele, M.; Santos, C. M.; Fai, A. E. C.; **Gonçalves, M. H.*; Shimizu, F. M.*;** Santos, M. S. dos; Moure, R. B.; Nascimento, D. D.; Guimaraes, A. L. de A.; Saint Clair, dos S. G.; Vicosa, A. L.; Cabral, L. M.

Background/Objectives: Pediatric drug administration is hindered by difficulties in swallowing conventional medications and the unpalatable taste of many drugs. Among diseases highlighting the need for improved pediatric delivery, tuberculosis (TB) stands out. One form of the disease is latent TB infection (LTBI), which is concerning in children. Effective LTBI treatment is crucial for prevention, with isoniazid (INH) widely used for its proven efficacy and safety. This study aims to develop innovative 3D-printed chewable gels containing INH for LTBI treatment. Methods: The gels were formulated using gelatin and carrageenan gum, sugar-free sweeteners, and flavoring. Two batches were prepared, and using 3D printing (3DP) with a semi-solid extrusion (SSE) module, chewable gels were produced. Rheological properties were measured to assess the feasibility of 3DP-SSE, evaluating the structural integrity and adequate fluidity of the formulation. The 3D-printed chewable gels were evaluated by visual, mass, and dimensional characteristics. In addition, the water activity, texture profile, INH and degradation product content, in vitro release, and taste-masking were investigated. Results: The optimized formulation maintained suitable rheological properties for 3DP-SSE, demonstrating consistent weight, dimensions, and stability after the process. The texture achieved a balance between printing parameters and shape maintenance, and the INH presented an immediate--release profile (>85% within 30 min). The chewable gels showed an improvement in palatability compared to conventional INH tablets. Conclusions: This innovative approach offers a promising solution for pediatric LTBI treatment, as it improves efficacy, medication acceptability, and on-demand access.

PHARMACEUTICS 17[5], 658, 2025. DOI: 10.3390/pharmaceutics17050658

[P128-2025] "Topological transitions, pinning and ratchets for driven magnetic hopfions in nanostructures"

Souza, J. C. B.; Reichhardt, C. J. O.; Reichhardt, C.; Saxena, A.; **Vizarim, N. P.*;** Venegas, P. A.

Using atomistic simulations, we examine the dynamics of three-dimensional magnetic hopfions interacting with an array of line defects or posts as a function of defect spacing, defect strength, and current. We find a pinned phase, a sliding phase where a hopfion can move through the posts or hurdles by distorting, and a regime where the hopfion becomes compressed and transforms into a toron that is half the size of the hopfion and moves at a lower velocity. The toron states occur when the defects are strong; however, in the toron regime, it is possible to stabilize sliding hopfions by increasing the applied current. Hopfions move without a Hall angle, while the toron moves with a finite Hall angle. We also show that when a hopfion interacts with an asymmetric array of planar defects, a ratchet effect consisting of a net dc motion can be realized under purely ac driving.

SCIENTIFIC REPORTS 15[1], 16802, 2025. DOI: 10.1038/s41598-025-01349-9

[P129-2025] "Tuning the Coherent Interaction of an Electron Qubit and a Nuclear Magnon"

Shofer, N.; Zaporski, L.; Appel, M. H.; Manna, S.; **Silva, S. C. da*;** Ghorbal, A.; Haeusler, U.; Rastelli, A.; Le Gall, C.; Gawetezyk, M.; Atatüre, M.; Gangloff, D. A.

A central spin qubit interacting coherently with an ensemble of proximal spins can be used to engineer entangled collective states or a multiqubit register. Making full use of this many-body platform requires tuning the interaction between the central spin and its spin register. GaAs quantum dots offer a model realization of the central spin system where an electron qubit interacts with multiple ensembles of similar to 104 nuclear spins. In this work, we demonstrate tuning of the interaction between the electron qubit and the nuclear many-body system in a GaAs quantum dot. The homogeneity of the GaAs system allows us to perform high-precision and isotopically selective nuclear sideband spectroscopy, which reveals the singlenucleus electronic Knight field. Together with time-resolved spectroscopy of the nuclear field, this fully characterizes the electron-nuclear interaction for a priori control. An algorithmic feedback sequence selects the nuclear polarization precisely, which adjusts the electron-nuclear exchange interaction in situ via the electronic g-factor anisotropy. This allows us to tune directly the activation rate of a collective nuclear excitation (magnon) and the coherence time of the electron qubit. Our method is applicable to similar central-spin systems and enables the programmable tuning of coherent interactions in the many-body regime.

PHYSICAL REVIEW X 15[2], 021004, 2025. DOI: 10.1103/PhysRevX.15.021004

[P130-2025] "Unassisted Photoelectrochemical CO2 Conversion into Liquid Products by a Light-Responsive Gas-Diffusion Electrode"

Alvim, J. C.; Soares, L. C.; Macedo, N. G.; Galante, M. T.; Sangali, M.; Caram, R.; **Siervo, A. de*;** Chansai, S.; Hardacre, C.; Longo, C.

The combination of suitable semiconductors as photoelectrodes could sustainably provide unassisted CO2 conversion using sunlight; however, few reports describe such achievement at this time. Herein, ethanol and formate were produced in a photoreactor assembled with a photoresponsive gas-diffusion electrode (GDE) containing Cu2WO4. The energy diagram, built from band gap energy and flat band potential (E-FB) values, shows that the position of the Cu2WO4 conduction band edge is suitable to promote CO2 reduction in different products. BiVO4 deposited on titanium foil was used as the photoanode; large-area Ti|BiVO4 was successfully synthesized from the Ti|BiOI template; additional deposition of FeOOH/NiOOH decreased E-FB and charge recombination, improving the photoanode performance for the O-2 evolution reaction. The CO2--fed GDE/Cu2WO4 (7.5 cm(2)) photocathode and the Ti|BiVO4/FeOOH/NiOOH (9.0 cm(2)) photoanode were assembled in a H-type reactor containing NaHCO3 aqueous solution. Under irradiation, these associated photoelectrodes supplied the thermodynamic requirements for a spontaneous current flow of 0.7 mA and, without any external bias, produced formate (16.5 mu g h(-1) cm(-2)) and ethanol (1.9 mu g h(-1) cm(-2)) at the cathode with solar-to-fuel efficiency of 0.07 and 0.005%, respectively. This photoreactor can be an inspiration for designing sustainable devices for CO2 valorization using sunlight.

ACS SUSTAINABLE CHEMISTRY & ENGINEERING, 2025. DOI: 10.1021/acssuschemeng.5c01227. Early Access Date: MAY 2025

[P131-2025] "Unexpected consequences of postquantum theories in the graph-theoretical approach to correlations"

Nogueira, J.*; Vieira, C.; Cunha, M. T.

This work explores the implications of the exclusivity principle (EP) in the context of quantum and postquantum correlations. We first establish a key technical result demonstrating that given the set of correlations for a complementary experiment,

the EP restricts the maximum set of correlations for the original experiment to the antiblocking set. Based on it, we can prove our central result: if all quantum behaviors are accessible in Nature, the EP guarantees that no postquantum behaviors can be realized. This can be seen as a generalization of the result of B. Amaral et al. [Phys. Rev. A 89, 030101(R) (2014)], to a wider range of scenarios. It also provides novel insights into the structure of quantum correlations and their limitations.

PHYSICAL REVIEW A 111[5], 052418, 2025. DOI: 10.1103/PhysRevA.111.052418

[P132-2025] "Unraveling Non-Cubic Atomic Ordering in Surfactant-Free AuAg Decahedral Nanoparticles by Pair Distribution Function (PDF) Analysis"

Corrêa, L. M.*; Moreira, M.*; Rodrigues, V.*; Ugarte, D.*

Atomic arrangement in decahedral (Dh) nanoparticles remains an open and contentious question. The well-accepted Bagley model predicts a homogeneous deformation of face-centered cubic (FCC) crystal into a body-centered orthorhombic (BCO) one, including a 5% expansion along the 5-fold axis. This BCO model is questioned by experimental evidence of localized deformations or observation of Dh wires with body-centered tetragonal lattice (BCT). Transmission electron microscopy (TEM) images may be used to detect strain fields, but 2D projection nature of images inhibits the complete assessment of 3D distortion fields. Here, the average unit-cell symmetry and size of few-nm-wide surfactant-free noble metal (AuAg) nanoparticles are studied using a structural refinement based on Pair Distribution Function (PDF) derived from Precession Electron Diffraction (PED). The results indicate that the Bagley BCO model is clearly unable to provide a good description, and that the occurrence of a tetragonal symmetry cannot be excluded within experimental errors. Structural refinement has followed rigorous uncertainty estimation and solution search procedures, considering physical constraints and a minimal number of variables. The PDF approach shows high potential to obtain information of the average unit cell in nanocrystals using low electron total irradiation dose (approximate to 10 e(-) /& Aring;(-2)).

PARTICLE & PARTICLE SYSTEMS CHARACTERIZATION, 2025. DOI: 10.1002/ppsc.202500031 Early Access Date: MAY 2025

[P133-2025] "Voltage-tunable spin resonance in quantum phase-separated material"

Gomide, G. B.*; Carranza-Celis, D.; **Kuhl, G.*; Knobel, M.***; Ramírez, J. G.; **Muraca, D.***

The voltage control of spin and charge degrees of freedom in complex materials is a cornerstone for the realization of advanced electronic devices with enhanced functionalities. Here, we demonstrate in situ indirect current control via the Joule effect of the spin resonance parameters in a phase-separated La5/8-y Pr y Ca3/8MnO3 sample while simultaneously inducing resistive switching. By employing electron paramagnetic resonance (EPR) spectroscopy under an applied bias voltage, we observe sharp, reversible modifications in the EPR spectra-linewidth, resonance field, and intensity-concurrent with voltage-driven transitions between the ferromagnetic metallic (FMM) and paramagnetic charge-ordered (PM-CO) states. This real-time probing of spin resonance during resistive switching provides crucial insights into the interplay between spin, charge, and lattice degrees of freedom, elucidating the distinct roles of the FMM and PM-CO phases in the observed behavior. These findings pave the way for the development of novel spintronic and neuromorphic devices with voltage-tunable functionalities.

APL MATERIALS 13[4], 041122, 2025. DOI: 10.1063/5.0256253

Eventos publicados

[P134-2025] "Modeling the impact of including the charge carrier creation and transport in photon counting detectors on the radiographic image formation"

Mendes, H. R.*; Tomal, A*
Sabol J. M.; Li K.; Abbaszadeh S.

Semiconductor detectors have increasingly been utilized in medical imaging, particularly in photon-counting detectors. Monte Carlo (MC) simulation is a valuable tool for studying the image formation process. However, common MC codes used in medical imaging detection simulations often simplify important factors, such as the crystalline structure. This study aims to quantify the impact on image quality when a more detailed MC code is employed. The PENELOPE code was used as a standard, while the THOR code, which models electron--hole pair (EHP) creation and transport, was utilized for comparison. The simulation setup includes a polyenergetic X-ray source (40-80 kV), a newborn anthropomorphic phantom, a carbon fiber table, and a 1 mm thick CdTe detector biased at -300 V. Image quality was assessed using contrast and signal--to-noise ratio (SNR). The THOR code produced images with 50% fewer counts due to EHP losses, particularly charge trapping, resulting in lower contrast and SNR compared to the PENELOPE code, with relative differences of up to 6.75% and 39%, respectively. This study presents the impact of a detailed modeling of semiconductor detectors and reveals how neglecting this model leads to an overestimation of image quality.

MEDICAL IMAGING 2025: PHYSICS OF MEDICAL IMAGING, PT 1, Progress in Biomedical Optics and Imaging 13405, 1340536, 2025. DOI: 10.1117/12.3048610

[P135-2025] "Monte Carlo simulation of photon-counting breast CT system: from implementation to image quality evaluation"

Tomal, A.*; Michielsen, K*; Pautasso, J. J.; Sechopoulos, I.
Sabol J. M.; Li K.; Abbaszadeh S. (Ed.)

Photon-counting detectors (PCD) are an emerging technology that has the potential to improve the image quality and material characterization capabilities in breast CT (bCT) compared to energy-integrating detectors (EID). This work focuses on implementing a Monte Carlo (MC) model to simulate PCD, using a previously validated Geant4-based MC code. MC simulations of bCT acquisitions, using both PC and EI detection technologies, were performed to investigate image quality improvement. To evaluate PCD simulation performance, a 50 keV beam was simulated with an energy threshold of 20 keV and four energy bins. The detection efficiency was 88%, with 24% of the counts corresponding to the incorrect energy channel due to partial energy deposition and charge-sharing effects. For image quality evaluation, projection images for bCT were simulated using anthropomorphic breast phantoms with an added iodinated spherical lesion and a W/Cu (0.257 mm) at 65 kV x--ray spectrum. 225 projections were simulated, and CT images were reconstructed using IMPACT method. Image quality was evaluated using the signal-to-noise ratio (SNR) and contrast--to-noise ratio (CNR). Comparing the simulated projections, the SNR and CNR increased, respectively, by up to 88/95% and 31/35% for single/multichannel PCD vs. EID. For the reconstructed images, the improvements were up to 27%/9%. It was observed a better accuracy and precision of linear attenuation coefficient estimation for PCD (PCD: 4.4% and 3.0%, and EID: 6.7% and 3.3%, on average, respectively). Overall, the PCD detector provides improved image quality and more accurate tissue characterization compared to the EID detector for bCT.

MEDICAL IMAGING 2025: PHYSICS OF MEDICAL IMAGING, PT 1, Progress in Biomedical Optics and Imaging 13405, 1340543, 2025. DOI: 10.1117/12.3048491

[P136-2025] "Pipeline to generate synthesized mammographic images: reliability of a new framework for data augmentation-based ray-tracing method, Monte Carlo simulation, and deep learning scatter estimation"

Machado, A. Y.*; Rodrigo, T. M.*; Tomal, A.*
Sabol J. M.; Li K.; Abbaszadeh S. (Ed.)

The generation of synthesized mammographic images is pivotal for the advancement of virtual clinical trials and the enhancement of machine learning models through data augmentation applied to breast imaging. In this study, it is presented a comprehensive framework that integrates Monte Carlo simulations, ray-tracing methods and deep learning model for scatter estimation to efficiently generate synthesized mammographic images. 311 anthropomorphic breast phantoms were utilized to produce a dataset of 6220 simulated images across different beam energies, which were used to train a deep learning model based on the ResNet architecture. The model achieved a mean absolute percentage error of 2.49 +/- 4.04% in scatter prediction compared to MC simulations, along with a structural similarity index measure of 0.98 +/- 0.02. Subsequently, a ray-tracing algorithm was employed to generate primary images from a compressed breast phantom in CC view, which were combined with deep learning scatter predictions to produce synthesized polyenergetic mammographic images. This approach significantly reduced computational time by an order of magnitude compared to traditional MC methods, enabling faster generation of synthesized images, compared to traditional methods. The proposed pipeline facilitates the creation of large and diverse datasets, supporting the optimization of image analysis and virtual clinical trials in mammography.

MEDICAL IMAGING 2025: PHYSICS OF MEDICAL IMAGING, PT 1, Progress in Biomedical Optics and Imaging, 13405, 1340545 DOI: 10.1117/12.3048533

Correções

[C001-2025] "Dielectron production in proton-proton and proton-lead collisions at √sNN = 5.02 TeV (vol 102, 055204, 2020)"

Acharya, S.; Adamova, D.; Agarwal, A.; **Chinellato, D. D.*; Guardiano, G. G.*; Liveraro, G. S. S.*; Takahashi, J.***; et al.
ALICE Collaboration

This is an addendum to the article "Dielectron production in proton-proton and proton-lead collisions at root s(NN) = 5.02 TeV" published in [Phys. Rev. C 102, 055204 (2020)]. We update the extracted charm cross section at midrapidity given in Table III and Fig. 4 (left) of the original publication with the fragmentation fractions of charm quarks in pp collisions published in [Phys. Rev. D 105, L011103 (2022)].

PHYSICAL REVIEW C 111[2], 024905, 2025. DOI: 10.1103/PhysRevC.111.024905

[C002-2025] "Search for a common baryon source in high-multiplicity pp collisions at the LHC (vol 811, 135849, 2020)"

Acharya, S.; Adamova, D.; Adler, A.; **Albuquerque, D. S. D.*; Chinellato, D. D.*; Takahashi, J.***; et al.
ALICE Collaboration

PHYSICS LETTERS B 861, 139233, 2025. DOI: 10.1016/j.physletb.2024.139233

***Autores da comunidade IFGW**
Fonte: Web of Science on-line (WOS)

Defesas de Dissertações do IFGW

[D009-2025] "Explorando Supercondutividade via Ressonância Magnética"
Aluno: Isadora Neme Ribeiro
Orientador: Prof. Dr. Ricardo Rodrigues Urbano
Data: 23/04/2025

Defesas de Teses do IFGW

[T007-2025] "Estudo de Materiais Magnéticos e Supercondutores com Técnicas de Espectroscopia de raios-X e Microondas"
Aluno: Marina Raboni Ferreira
Orientador: Prof. Dr. Narcizo Marques de Souza Neto
Data: 06/06/2025

[T008-2025] "Alinhamento de spin de mésons e polarização de bárions usando modelo de coalescência fora do equilíbrio entre spin e vorticidade"
Aluno: Kayman Jhosef Carvalho Gonçalves
Orientador: Prof. Dr. Donato Giorgio Torrieri
Data: 04/07/2025

Fonte: Portal IFGW/Eventos
Disponível em: https://portal.ifi.unicamp.br/a-instituicao/eventos/month.calendar/2025/04/16/-

Abstracta

Instituto de Física Gleb Wataghin
Diretor: Prof. Dr. Marcos Cesar de Oliveira
Universidade Estadual de Campinas - UNICAMP
Cidade Universitária Zeferino Vaz
13083-859 - Campinas - SP - Brasil
e-mail: secdir@ifi.unicamp.br
Fone: +55 19 3521-5300

Publicação

Biblioteca do Instituto de Física Gleb Wataghin
http://portal.ifi.unicamp.br/biblioteca
Instagram: @bif.unicamp

Diretora Técnica: Sandra Maria Carlos Cartaxo
Coordenadora da Comissão de Biblioteca: Profa. Dra. Arlene Cristina Aguilar

Elaboração e editoração:
Maria Graciele Trevisan (Bibliotecária)
Contato: infobif@ifi.unicamp.br